RL-TR-95-170
Final Technical Report
September 1995

SIMULATION AND EVALUATION OF AN ANTENNA POLARIZATION NULLING PROCESSOR

LJR, Inc.

APPROVED FOR PUBLIC RELEASE; DISTRIBUTION UNLIMITED.

Rome Laboratory
Air Force Materiel Command
Griffiss Air Force Base, New York

This report has been reviewed by the Rome Laboratory Public Affairs Office (PA) and is releasable to the National Technical Information Service (NTIS). At NTIS it will be releasable to the general public, including foreign nations.

RL-TR-95-170 has been reviewed and is approved for publication.

APPROVED: Richard N. Smith

RICHARD N. SMITH
Project Engineer

FOR THE COMMANDER: John A. Graniero

JOHN A. GRANIERO
Chief Scientist
Command, Control & Communications Directorate

If your address has changed or if you wish to be removed from the Rome Laboratory mailing list, or if the addressee is no longer employed by your organization, please notify RL (C3BA) Griffiss AFB NY 13441. This will assist us in maintaining a current mailing list.

Do not return copies of this report unless contractual obligations or notices on a specific document require that it be returned.

REPORT DOCUMENTATION PAGE

Form Approved
OMB No. 0704-0188

1. AGENCY USE ONLY (Leave Blank)	2. REPORT DATE	3. REPORT TYPE AND DATES COVERED
	September 1995	Final Jun 94 - Jun 95

4. TITLE AND SUBTITLE
SIMULATION AND EVALUATION OF AN ANTENNA POLARIZATION NULLING PROCESSOR

5. FUNDING NUMBERS
C - F30602-94-C-0170
PE - 33110F
PR - 4056
TA - 01
WU - 05

6. AUTHOR(S)
N/A

7. PERFORMING ORGANIZATION NAME(S) AND ADDRESS(ES)
LJR, Inc.
360 North Sepulveda Boulevard
Suite 2030
El Segundo CA 90245

8. PERFORMING ORGANIZATION REPORT NUMBER
N/A

9. SPONSORING/MONITORING AGENCY NAME(S) AND ADDRESS(ES)
Rome Laboratory (C3BA)
525 Brooks Rd
Griffiss AFB NY 13441-4505

10. SPONSORING/MONITORING AGENCY REPORT NUMBER
RL-TR-95-170

11. SUPPLEMENTARY NOTES
Rome Laboratory Project Engineer: Richard N. Smith/C3BA/(315) 330-7436

12a. DISTRIBUTION/AVAILABILITY STATEMENT
Approved for public release; distribution unlimited.

12b. DISTRIBUTION CODE

13. ABSTRACT (Maximum 200 words)

The use of antenna polarization as a means of suppressing intentional and unintentional interference is investigated. An antenna polarization nulling algorithm is derived. The algorithm is implemented using computer simulation. The performance of the algorithm is evaluated using the simulation and the results presented in this report.

14. SUBJECT TERMS
Antennas, Polarization, Nulling, Communications

15. NUMBER OF PAGES
64

16. PRICE CODE

17. SECURITY CLASSIFICATION OF REPORT	18. SECURITY CLASSIFICATION OF THIS PAGE	19. SECURITY CLASSIFICATION OF ABSTRACT	20. LIMITATION OF ABSTRACT
UNCLASSIFIED	UNCLASSIFIED	UNCLASSIFIED	UL

TABLE OF CONTENTS

Simulation And Evaluation Of An Antenna Polarization Nulling Processor

I. INTRODUCTION

An antenna polarization nulling (APN) processor suppresses interfering signals by adjusting the receiving antenna's polarization such that the antenna rejects jamming signals while still receiving user signals. When a jammer varies the polarization of its radiated signals, the user's signal will vary due to a varying polarization mismatch. In general, the user's signal amplitude will vary less than 10 dB, 90% of the time. Use of a diversity waveform and error correction coding can eliminate errors due to the fading-like phenomena produced by this variation in the user's signal amplitude. When the user's signal is at least 10 dB greater than its receiver's thermal noise (SNR > 10 dB), APN can reduce the jamming signals more than 30 dB. This occurs even when the user and jammer signal sources are collocated. Since all signals incident on the receiving antenna add to produce a single field, APN can suppress all incident interfering signals simultaneously.

Adaptive nulling antennas use spatial discrimination as a means for suppressing jammer signals, while reducing gain to user terminals a tolerable amount. This process requires an electrically large antenna aperture. The required antenna aperture is practical at EHF and barely tolerable at SHF. At UHF, it is virtually impossible to place the required antenna aperture on a spacecraft and launch it.

Spread-spectrum waveforms are also used to suppress jamming signals. However, higher data rate communication systems usually do not have sufficient operating bandwidth to suppress expected jammer threats. Nevertheless, it is wise to always use an AJ waveform if interference is expected. APN can be used in addition to a spread-spectrum waveform and any existing spatial discrimination processors.

Thus, spatial discrimination requires a large antenna aperture, and temporal discrimination requires a large frequency bandwidth—neither of which are available in sufficient quantity at UHF and, possibly, at SHF. APN requires a large SNR ($\approx$ 10 dB) and a robust diversity and error correction processor. Although APN is perhaps most useful at UHF where the other AJ measures are, in effect, not available, it can operate at any RF frequency. It is fundamentally limited to operating at data rates less than 10 Mbps, or to service a large community of users whose total data rate is less than $\approx$ 10 Mbps.

This Report describes the details of and APN algorithm, and a communication simulator designed to demonstrate its performance. It also presents the results of a statistical analysis of the expected bit error performance in the presence of sensor errors. An example of the latter Study is shown in Figure 1, where the probability of an error in the detection of a bit is plotted versus the interfering signal's polarization angle, θ_j—the solid curve for operation with, and the dashed curve for operation without, APN. These results are for a jammer occupying the same frequency band

as the user, and with the amplitude equal to the user's amplitude. They will be discussed in detail in Section III of this Report.

Note that for a jammer polarization angle, $\theta_j < 72°$, the probability of a bit error occurring is less with APN that without APN. This improvement in performance is substantial as the jammer's polarization approaches that of the user. On the other hand, using APN increases the probability of a bit error when the jammer's polarization angle, θ_j, is greater than 72°. This might be expected as θ_j approaches the user's cross-polarization. It is indeed fortunate that for $\theta_j > 72°$, the probability of a bit error is less than 0.27 and as small as 0.02. Assuming θ_j is uniformly distributed, the probability of a bit error is less than ≈ 0.1 with APN versus 0.2 without APN. For those cases where θ_j is not uniformly distributed, it is likely that using APN results in a much less (or slightly higher) BER than without APN. When it is higher, the BER with APN is a maximum of 0.32 and it is usually less than 0.1. It is important to note that the curves shown in Figure 1 assumes that the jammer's signal amplitude equals the user's amplitude ($S/J = 0$ dB) and up to a 2 dB error in estimating the user's signal amplitude, A_u, and the jammer's signal amplitude, A_j, and up to an error of $\pi/8$ in estimating the user's polarization angle, θ_u. If A_j, A_u, and θ_u are known exactly, using APN eliminates all bit errors. The estimate of these signal parameters will be discussed later.

This Report addresses the fundamentals of APN in Section II. It is shown that suppression of interfering signals requires knowledge of the interfering signal's amplitude, user's signal amplitude, and the incident user's signal polarization. In Section III, the effect of error in determining these parameters is analyzed, with respect to producing and determining an error in detecting a QPSK bit. Results obtained with a computer simulation of an APN processing a QPSK waveform are presented in Section IV. Section VII presents a summary of this Program and its results. Recommendations for further development of an APN are presented in Section VIII.

Prior to describing the efforts and results of this Program, it is important to list the objectives, scope, and tasks as they appear in the associated Statement of Work (SOW); specifically:

> 1.0 Objective: This effort shall investigate Antenna Polarization Nulling (APN) technology and evaluate the performance capability of the Antenna Polarization Processor (APP). The APP shall consist of a computer simulation of an Antenna Polarization Nulling Algorithm (APNA). The effort shall develop the algorithm with practical application in suppressing incidental and intentional interference sources. The APP shall operate in a Military Satellite Communications (MILSATCOM) environment, at Ultra High Frequency (UHF) with date rates ranging from 64 Thousands of bits per second (Kbps) to several Millions of bits per second (Mbps).
>
> 2.0 Scope: This effort shall include four (4) major tasks. In particular, an APP will be defined, modeled, and implemented. using computer simulation. Several user signal and interference signal generators shall be defined, modeled, and implemented as part of the APP. The APNA shall process the user and interference signals so that the resulting interference suppression can be evaluated. The performance of the APP will be compared to conventional interference nulling/canceling processors. A performance measure shall be established and used to measure the APNA's performance.
>
> 4.1.1 Design of the APNA
>
> 4.1.1.1 Design an algorithm based on APN technology which shall be capable of nulling intentional and unintentional interference. The design shall include all algorithm

components required at both ends of the communication link. This includes the polarization modulation at the transmit end of the link and the polarization demodulation and interference nulling at the receive end of the link. The APNA shall be designed to operate in a MILSATCOM environment, at UHF with data rates ranging from 64Kbps to several Mbps.

4.1.1.2 Prepare an interim technical report documenting task 4.1.1 (Design of the APNA). (See CDRL, A002, and A003).

4.1.2 Implementation of APP

4.1.2.1 Implementation of the APP shall include simulation of the APNA on a processor/computer, simulation of all interference signals, simulation of satellite channel effects, simulation of all synchronizationís [sic] and modulations, generation of simulated data for transmission on the link and a means to verify APP operation.

4.1.2.2 Prepare an interim technical report documenting task 4.1.2 (Implementation of the APP). (See CDRL, A003, A004).

4.1.3 Evaluation of APP Performance

4.1.3.1 Evaluate performance of APP using a verity [sic] of scenarios. Vary all key parameters such as: the number of interference signals, type of interference signals, power of interference signals. power and characteristics of communications signal and effect of satellite channel. Also, vary APNA parameters to identify optimum performance values and configurations. Compare measured performance to conventional interference nulling techniques such as: Adaptive Array Nulling and Spread Spectrum techniques.

4.1.4 Figure of Merit/Performance measure

4.1.4.1 Develop a Figure of Merit/Performance measure which is an analytical method of evaluating APP and adaptive antenna performance of which dissimilar antennas and processors can be evaluated with reference to a particular requirement.

4.1.4.2 Document all technical work accomplished and information gained during the performance of this acquisition. This shall include all pertinent observations, nature of problems, positive as well as negative results, and design criteria established, where applicable: also procedures followed, processes developed, "Lesson Learned", etc. The details of all technical work shall be documented to permit full understanding of the techniques and procedures used in evolving technology of processes developed. Separate design, engineering, of process specifications delivered during this acquisition shall be cross-referenced to permit a full understanding of the total acquisition. (See CDRL, A005).

4.1.5 Continually determine the status of the effort and report progress toward accomplishment of contract requirements. (See CDRL, A001).

4.1.6 Conduct oral presentations at such times and places as designated in the contract schedule. These presentations shall provide the status of the technical progress made to date in the performance of the contract. The presentation will be attended by approximately eight (8) Government personnel and shall not exceed eight (8) hours, each. (See CDRL, A003).

DMH/jer

II. ANTENNA POLARIZATION NULLING

Antenna polarization is often described as ***vertical linear*** (VL), ***horizontal linear*** (HL), ***right-hand circular*** (RHCP), or ***left-hand circular*** (LHCP). In general, this is adequate for most communication and radar system designers and specification writers. It is customary to specify

the axial ratio of circularly polarized signals and the angular orientation of linearly polarized signals. These polarizations represent a very small subset of the vast number of polarizations that can exist. For example, the instantaneous polarization of signals radiated from the sun vary randomly over all polarizations than can be defined. It is also true that any polarization has a cross, or orthogonal, polarization. These pairs of polarizations form a set and are usually referred to as a pair of ***orthogonal polarizations***.

The Poincarre sphere (see Figure 2) is a common method of representing all polarizations. The sphere can be defined such that RHCP and LHCP are located at the poles of the sphere, as shown in Figure 3. In this case, all orientations of linear polarization are located on the Equator of the sphere and all elliptical polarizations are located elsewhere on the sphere. Thus, the sphere represents all possible polarizations of any electromagnetic field. It also has some special characteristics that help in describing APN. Specifically, orthogonal polarizations are located diametrically opposite one another, and the coupling between waves with different polarizations is equal to $\cos^2(\beta/2)$, where β is the angle between radial vectors terminating on the two polarizations. For example, for orthogonally polarized fields $\beta = 180°$ and the coupling = 0, as expected.

In the remainder of this Report (and in Appendix A) the North and South poles of the Poincarre sphere represent VL and HL, respectively. This does not effect the generality of the analysis; it renders the mathematics somewhat less complicated and improves a physical interpretation of the APN concepts. A standard right-hand spherical coordinate system is used with HL polarization located at $\theta = 0$, and with VL polarization located at $\theta = \pi$. The related mathematics is presented in Appendix A.

In its most advanced form, APN will operate with the user terminal varying the polarization of its radiated signals in a random but known (only to the intended receiver) fashion. This will prevent an interferer from transmitting noise with a polarization identical to that of the user. An APN processor receives signals via a pair of orthogonally polarized collocated antennas. These signals are weighted (their phase and amplitude are modified) and summed to suppress the interfering signals. That is, the processor adjusts the polarization produced by the pair of antennas such that it is orthogonal to the polarization of the total interfering signal, E_j. Note that E_j can be produced by a single interfering source, or several incoherent, or coherent, sources. It is a single field added to the user's incident signal, E_u, to form the total incident signal, E_t. In order to perform this function, an APN processor must know the polarization, P_u, and amplitude, $|E_u|$, of the user's signals and the amplitude of the interfering signals, $|E_j|$. It will be shown that the estimate of P_u and $|E_u|$ can be less accurate than the estimate of $|E_j|$. In the interest of the anxious reader, the data shown in Figure 1 was calculated with the estimate of $|E_j|$ and $|E_u|$ within 2 dB of their actual values and β_u, the angle between the actual user's polarization, P_u, and the estimated value of P_u, less than $\pi/8$.

Note that the user's signal is also reduced as the antenna's polarization is varied to suppress the interfering signals. That is, the amplitude of a received signal power, P_r, can be represented by:

$$P_r = A\cos^2(\beta/2)S, \tag{1}$$

where S is the incident signal power flux density and A is the antenna's effective absorption area. Using (1), and assuming the incident interfering signal polarization will be uniformly distributed over all polarizations, the user's received power, P_{ru}, will be suppressed less than a factor, α, with probability greater than 1-α. In other words, the user's signals will be reduced less than 10 dB, 90% of the time. For example, if the user's signal–to–thermal-noise ratio (SNR) is greater than 15 dB, an APN processor will suppress the interfering signals and the user's SNR will be > 5 dB, 90% of the time. The interfering signals will be suppressed more than 30 dB if the estimate of $|E_j|$, $|E_u|$, and P_u are sufficiently accurate. A forward error correction algorithm will most likely recover bit errors that occur during those periods when the user's SNR is inadequate.

In its simplest form, an APN estimates $|E_j|$ by first measuring the power received with the antenna's polarization set to the user's (or estimated user's) polarization. Assuming P_u is known, power P_x, received with the antenna's polarization set to P_{ux}, the user's cross-polarization, will be given by:

$$P_x = |E_j|^2 \cos^2\left(\frac{\theta_{mj}}{2}\right), \tag{2}$$

where θ_{mj} is the angle between the jammer's polarization angle, θ_j, and the user's cross-polarization angle, θ_{xu}. Thus, assuming a value of $|E_j|^2$, θ_{mj} can be calculated using (2). Since we have assumed $\theta_u = 0$, the jammer's cross-polarization angle, θ_{xj}, equals π-θ_{mj}. This relationship is shown in Figure 4. Note that finding θ_{xj} defines the circle on the polarization sphere that contains P_{xj}; it remains to determine the value of ϕ_{xj} that uniquely defines the interfering signal's polarization.

Recall that when the antenna's polarization is set to P_{xj}, only the user's signal will be received. For any antenna polarization different from P_{xj}, the total signal received depends on the signal phase, ζ, between the jammer's and user's signals. Diagrams in Figure 4 indicate the variation in the total signal received as the polarization angle, ϕ_{xj}, is varied over its entire range of 0 to 2π radians when $\theta = \theta_{xj}$. When $\zeta = 0$ or 180°, there is only one point on the circle where the total received signal magnitude equals the estimated user signal amplitude. For all other cases, there are two values of ϕ_{xj} that will give a signal amplitude equal to the expected user signal amplitude. This is what gives rise to the two solutions for γ in (3). The graph in Figure 4 indicates the variation in signal received at the antenna output as ϕ_{xj} is varied over its range or as the polarization of the antenna is varied along the circle that contains P_{xj}. It is at this point that analysts have indicated that it is not possible to pick the correct value of ϕ_{xj}; hence, an APN processor will fail to implement the desired polarization.

The correct value of ϕ_{xj} can be determined by using both solutions to determine the received information bit. In this case, the bit must be either 0°, 90°, 180°, or 270°. The algorithm selects that bit which yields a minimum ξ_e, the phase difference between the phase of the detected bit and the four expected bits. When $|E_u|$, $|E_j|$, and θ_u are without error ($\xi_e = 0$), the correct ϕ_{xj} is always selected and the interfering signals are suppressed more than 30 dB.

An estimate of $|E_j|$ can be improved by using ξ_e and the selected received bit to calculate a new value of $|E_j|$—assuming error-free estimates of $|E_u|$ and θ_u, the user's signal amplitude and

polarization angle, respectively. In Section III, the sensitivity of selecting the correct bit will be examined as a function of the error in estimating $|E_j|$, $|E_u|$, and θ_u. Surprisingly large errors in these quantities are tolerable. Future studies of an APN processor can improve the primitive feedback loop described here so that expected variations in $|E_j|$, the most sensitive parameter, can be predicted or anticipated.

Before discussing the sensitivity of errors in estimating the three uncertain APN processor parameters, it is important to display the simplicity of the algorithm's mathematics, in contrast to the complexity of its derivation (see Appendix A) and the conceptual discussion given in the foregoing. Referring to Equation (38) in Appendix A, γ, the phase of the user's received signal, is given by:

$$\gamma = \alpha_c \pm \cos^{-1}\left[\frac{a^2 + |t_c|^2 - n_c^2}{2a|t_c|}\right]. \tag{3}$$

With the antenna's polarization set equal to P_u, the assumed user's polarization, α_c and $|t_c|$ are the phase and amplitude of the signal received at the antenna's copolarized port, a is the estimated user's amplitude, and n_c is the magnitude of the jammer's signal received at the antenna's copolarized port. Note that n_c is calculated from:

$$n_c^2 = |E_j|^2 - n_x^2, \tag{4}$$

where n_x^2 is the power received at the antenna's cross-polarized port and $|E_j|^2$ is the estimate of the interfering signal's power. The second term on the right side of (3) introduces the uncertainty in calculating the correct value of γ. Note that when there is not an interfering signal present, $n_c = 0$, $|t_c| = a$, and the second term reduces to 0, as it should.

Note that only two calculations are required; they are indicated by (3) and (4). The resulting values of γ must be compared to γ_e, the expected values of γ. The expected value most nearly equal to γ is selected as the transmitted bit, γ_0. Then, a better estimate of n_c^2 is obtained by substituting γ_0 for γ in (3) and solving for a new value of n_c^2. Using (4), a new value of $|E_j|^2$ can be calculated. The latter is used in calculating γ for the next transmitted bit.

The foregoing algorithm and a simulation of its use as a processor is indicated in Figure 5. In the upper left corner, user and jammer signal generators produce signals that are polarized and then combined as a single signal. In the simulator, described latter in Section IV, the user's signal amplitude and polarization are held constant while the jammer's amplitude and polarization are varied. The combined signal is filtered and down-converted to represent a received signal in the presence of jamming. This signal is sampled and held to convert the incident signals to a digital representation. The APN algorithm uses an estimate of the user's signal amplitude and polarization and the jammer's amplitude to calculate the two values of γ as described in (3). These values are compared with the expected values—one of which is selected. The selected value is then used to calculate an improved estimate of the jammer's signal amplitude.

Note that the simulator does not have a phase-locked loop (PLL) as would be used by a QPSK signal demodulator. Rather, a sample of the user's signal frequency was used to synchronize the

detector to avoid the errors that would be introduced by a less-than-perfect PLL. It was felt that the thrust of the Study was to evaluate an APP, as opposed to develop a suitable PLL.

III. Sensitivity to Error in Parameter Estimates

Recall that an APN algorithm uses three estimates in calculating the phase of the transmitted bit and adjusts the antenna's polarization to be orthogonal to the incident interfering signal's polarization. These APN estimate parameters are:

1. User signal amplitude;
2. User signal polarization; and
3. Jammer signal amplitude.

Error sensitivity in the above three parameters were investigated by first assuming an error in one parameter with the other parameters error-free, then calculating the probability of an error in the detected phase of a bit. The calculation assumed a fixed value of θ_j and assumed a uniform distribution of ϕ_j, the jammer's other signal polarization angle, and ζ, its time phase relative to the user's signal time phase. The jammer's and user's signal amplitudes were allowed to vary up to 6 dB above and 6 dB below their error-free values. The user's signal polarization was allowed to vary over the range of $-\pi/4$ to $\pi/4$. The resulting error sensitivities are shown in Figures 6a–6c for a user's signal-to-jammer amplitude ratio (S/J) equal to 0 dB. The data shown in Figures 7a–7c are for $S/J = 3$ dB. A similar set of plots are shown in Figures 8a–8c and 9a–9c, for operation without the use of APN.

The decimal annotation (Figures 6a–9c) in each shaded region indicates the fractional number of bit errors that occurred for the range of ϕ_j and ζ used. That is, a total of 324 values of ϕ_j and ζ were used to calculate the detected bit's phase. For each θ_j, $|E_j|^2$, θ_u, and $|E_u|^2 = \alpha^2$, the number of bit errors (BEN) was calculated and divided by 324, the total number of samples. The plots in Figures 6a–9c were prepared by computing the BEN for points at the intersection of the grids on each Figure. The shaded contours were derived from these points.

These plots indicate that the error in estimating the jammer's amplitude causes the largest increase in producing an error in detecting the phase of a bit. It also shows that using APN reduces the probability of an error in the phase of a bit from that obtained without the use of APN in those cases when the jammer's power is underestimated and when the user's signal amplitude and polarization are in error. Note that when the jammer's amplitude is known within ≈ 1 dB, use of APN always results in performance superior to that obtained in the absence of APN.

The data shown in Figures 6a–9c is helpful in identifying the accuracy needed in estimating the APN parameters. A more informative calculation of the probability of an error in detecting the phase of the transmitted signal can be obtained by combining the error probability distributions for all three APN parameters and computing the probability of detecting the phase incorrectly. This calculation was carried-out using the probability density functions shown in Figures 10a and 10b. Note that the user's and jammer's signal amplitude estimate errors are assumed to have a Ricean distribution, P_A. That is, it is assumed that signal amplitudes greater than the estimated value is less likely to occur than if they are less than the estimated value. The most likely signal amplitude

is equal to the estimated value. The maximum and minimum values are 2 dB more and 2 dB less than the estimated value. This distribution is shown in Figure 10a.

The user's signal polarization angle, θ_u, was assumed to have a Guassian distribution, P_θ, centered on $\theta_u = 0$, the estimated value of the user's signal polarization angle. This distribution is shown in Figure 10b. Note that θ_u is assumed to be between -22.5° and 22.5°.

The probability, $\mathrm{Pe}(\theta_j)$, of an error in detecting the phase of a bit error was computed using:

$$\mathrm{Pe}(\theta_j) = \sum_m^M A_u P_A \sum_n^N A_j P_A \sum_r^R \theta_u P_\theta \sum_s^S \phi_s \frac{1}{S} \sum_t^T \zeta_t \frac{1}{T} \tag{5}$$

where A_u, A_j, and θ_u are the errors in estimating the amplitude of the user's signal, the amplitude of the jammer's signal, and the user's signal polarization angle, respectively. The jammer's second polarization, ϕ_s, and its time phase, ζ_t, are assumed to be uniformly distributed over 2π radians; that is:

$$\phi_s = \frac{2\pi s}{S} \tag{6}$$

$$\zeta_t = \frac{2\pi t}{T} \tag{7}$$

where S and T are both equal to 18. Thus, ϕ_s and ζ_t have a probability of $1/S$ and $1/T$, respectively.

$\mathrm{Pe}(\theta_j)$ was computed using (5) for $\theta_j = \frac{\pi}{10}, \frac{\pi}{5}, \cdots, \frac{9\pi}{10}$ and $S/J = 0$ dB and -3 dB. The computation of (5) was carried-out with and without APN while assuming the same user's polarization estimate for both cases. It is important to recognize the APN can change the estimate of the user's polarization to improve performance in those cases where the jammer's polarization angle, θ_j, is not randomly distributed. For example, when θ_j is slowly varying or fixed, APN can anticipate the future values of θ_j and improve its AJ performance. The results shown in Figure 11a indicate that with APN the maximum P_e is less than 25%, whereas without APN, P_e can approach 50%. The results also indicate that, when $\theta_j > 72°$, P_e is greater with APN than without APN.

The results shown in Figures 11a and 11bare very helpful in indicating the expected performance of APN. However, these results were obtained using assumed errors in estimating the three APN parameters. If the error in the jammer's signal amplitude is reduced to less than 1 dB, using APN will result in a smaller value of P_e, for all values of θ_j, than if APN is not used.

It is important to note that the P_e indicated in Figure 11a is based on assumed jammer and user characteristics that were selected as a best guess of what might be worst, or at least, bad estimates of the three APN parameters. Further development of an APNA is sure to improve the accuracy in estimating these parameters. For example, the APN algorithm calculates θ_j, the jammer's polarization angle. A simple modification of the APN would select the APN-derived transmit bit if $\theta_j < 72°$ and select the non-APN–derived bit for $\theta_j > 72°$. Still further, a historical record of

these parameters could improve the estimate used by APNA. This will certainly reduce P_e to a value less than ≈ 0.25 for all θ_j. Forward error correcting methods could be used to reduce the BER, as with other communications systems. Consultation with a communications specialist indicate that with practical coding, a BER $< 10^{-5}$ can be readily achieved if the symbol error rate is less than ≈ 0.27.

IV. APN Simulator

This Section describes a personal computer simulation of an APP, summarizes the results, and addresses Paragraph 4.1.2 of the Statement of Work. A block diagram of the simulator is shown in Figure 12. The transmitter generates a QPSK-modulated RF signal that is passed to a horizontally polarized "radiator." A similar RF signal generator's output was divided and incoherently modulated with random signals. These signals were passed to a horizontally polarized (HL) "radiator" and a vertically polarized (VL) "radiator." In order to keep the simulation free of non-related mechanisms, these signals were not radiated—they were passed directly to the ports of a receiving HL and VL "antenna," respectively. Note that the user's and jammer's HL signals were combined prior to being sent to the "receiver."

Still referring to Figure 12, the "separator" resolves the signal into in-phase (I) and quadrature-phase (Q) signals from the HL and VL signal ports. The "sample-and-hold" function converts these analog signals to a digital representation and passes them to the APN processor (APNP). The APNP reduces the jammer's amplitude and detects the phase of the received bit. This is compared to the known transmitted bit and any errors are counted. This count is used to measure the bit error rate (BER) of the processor.

The synchronizer adjusts the signal delays introduced by the simulator so that the APNP processes the chips as groups that form a bit. The "power calculator" is used to monitor the recovered power and enable a diagnosis of the performance of the simulator.

This simulator uses MATLAB software and includes a Simulink communications processor manufactured by The MathWorks, Inc. The software was designed to be capable of overall construction by assembling several modules to realize the desired processor. Unfortunately, each module has its own unique, and sometimes unexpected, performance characteristics. The unexpected abnormal behavior of this software caused several problems and required a substantially longer time to produce a satisfactory simulator.

Each block diagram in Figure 12 is "expanded" in Figures 12a–12d. Note that there is not a phase-locked loop (PLL); it was much too difficult to configure this simulator with an available PLL and make it perform unambiguously with the other components. It was felt that the APNP was the main block of interest and the only additional blocks should be those necessary to generate the desired signals. In fact, at a late date it was recognized that the signals out of the sample-and-hold function could have been saved directly to a file. Then, using computer code similar to that code that produced the results given in the previous Section, the digitized signals could have been processed just as an operational APN might process them. Unfortunately, time did not permit this to be implemented. Nevertheless, some meaningful data was obtained using the simulator shown in Figure 12.

When the user's power (as measured by the power calculator) was set equal to 1 Watt, the jammer's power was set to have a nominal value of 1 Watt and was either: (1) held constant; (2) varied sinusoidally up to ≈ 2 dB; or (3) varied randomly up to ≈ 2 dB. At the same time, the jammer's signal polarization angles were varied randomly over π radians, or held fixed. Thus, jammers with varying amplitudes and polarizations were studied.

For a typical test, 100 bits were sent and detected. These detected bits were compared with the transmitted bit to accumulate the number of errors. This was done for operation with and without the APNP enabled. The results are given in Table I. The first column in the table lists the amplitude of the randomly varying jammer's signal at the transmitter. The actual jammer's signal power is given in columns 5 and 6. Columns 2 and 3 describe the variation in jammer polarization and column 4 describes the rate over which the variation occurs. The performance of the simulation, both with and without APN, is given in the two right-most columns. The data rate was 2400 bps.

Referring to Table I, note that with the jammer's amplitude held constant ($A_0 = 0$ V), APN quickly finds the jammer's amplitude and reduces the BER to less than 1%. Time did not permit longer runs to determine a more accurate BER. Suffice it to say, APN substantially reduces the jammer's signal and all but eliminates bit errors. In other words, a relatively constant amplitude jammer can readily be suppressed by an APN processor, even one as primitive as the one developed during this Study. This type of jammer is commonly used to jam a band-limited transponder channel. It is common that the jammer will transmit a tone within the channel with intent to saturate the transponders amplifier and increase the channel's noise level through intermodulation distortion and/or small signal suppression. Whether or not this type of jammer varies its polarization or keeps it fixed, an APNP will easily identify the jammer's polarization and suppress its signals, even if the polarization is varied at the communication data rate. Of course, this assumes that an APNP can operate at speeds comparable to the data rate. This will be discussed in the next Section.

As the jammer varies its signal amplitude, the bit error increases. For example, with a 2 dB peak-to-peak variation in jammer amplitude, use of APN will reduce the BER compared to that obtained without APN. If the jammer's amplitude variation is increased to ≈ 3 dB, then the use of the APN algorithm used in this Study does not appear to be justified. However, the algorithm was not designed to use historically generated data, or different methods of sampling the signals. For example, the simulator used five chips per bit in order to use the software as it was designed. The algorithm used only the third chip in a bit instead of several chips. Using the additional chips will improve performance. The magnitude of this performance improvement is not known.

In summary, the simulator verifies the need to estimate the jammer's signal amplitude within a few dB, in agreement with the sensitivity analysis presented in the previous Section. The simulator clearly shows that the current algorithm can readily identify the jammer's amplitude if it varies at a rate slower than about one-half the communications data rate.

Quite aside from the simulator's ability to perform as an APNP, the detector module's performance was checked by determining BER as the signal-to-noise ratio (S/N) was varied from 0 to 8 dB and compared to the theoretical BER for a QPSK modulation. These results are shown in Figure 13.

V. Related Issues

This Study considered only a 2400 bps data rate, QPSK modulation, and continuous, as opposed to pulsed, jammers. These issues will be addressed in this Section by applying information gained from the Study. This will be followed by "lessons learned."

An APN processor requires an analog-to-digital converter (ADC) as it is presented in this Study. The speed and accuracy of this device will depend on the data rate and the desired signal suppression. It is expected that a 10-bit ADC operating at twice the data rate will be more than adequate. ADC's that have 12-bit accuracy and operate at several million samples-per-second (Msps) are readily available for less than $200. They could be made space-qualified and used in most any COMSAT. It is possible to obtain other ADC's that operate at 50 Msps that are less than ≈ $100,000. It will cost probably a few $100,000 to make them space-qualified. Thus, it is entirely possible than an ADC can be obtained to operate within APNP, handling up to ≈ 25 Mbps.

The APN algorithm used in this Study required only 20 lines of computer code that could complete detecting a bit in less than 20 μsec. It appears that the equivalent of a 100 MHz Pentium processor can handle up to a 1.5 Mbps data rate. Using buffers and parallel processors, it is likely that at least a 25 Mbps data rate can be handled by an APNP.

The current APN algorithm incorporates a QPSK detector. The logic for this detection could be used to demodulate any digital modulation, such as QPSK, BPSK, DPSK, M-ary FSK, and similar modulation waveforms. It is not designed to detect analog modulations such as FM or AM.

Since the APNP operates on instantaneous signals, it cannot be disrupted by a pulse, partial band, or similar types of jamming waveforms. That is, the APN algorithm samples and processes instantaneous signals. The three APN parameters are estimated using general knowledge and/or historical data. If a jammer chooses to radiate in discontinuous bursts, this information can be incorporated in the process of estimating the three APN parameters.

VI. Lessons Learned

Design and construction of any simulator requires somewhat arbitrary decisions concerning the processors that should and must be included in the simulator. In designing the APNP, it was first decided to include a phase-locked loop (PLL) as part of the signal demodulator. It was also decided to use MATLAB software for assembling signal processing simulators. After considerable effort, it was decided that:

1. Building a PLL using the MATLAB software was, in itself, a formidable effort;
2. Incorporating the APNP into the PLL was next to impossible; and
3. Time required to accurately measure BER far exceeded available time.

Significantly more information could be derived from using the simulator to generate a file containing typical received signal data generated by the simulator and processing it using computer code designed to perform APN and signal demodulation. That is, it was realized that an APNP should perform the signal detection so that the detection process can aid in determining the three APN parameters. Since APN requires a digital processor, it is much more logical to include

the system's signal demodulator as part of an APNP simulator; it will naturally be a part of any APNP.

The sensitivity analysis clearly demonstrates the accuracy required in estimating the three APN parameters. It appears that estimating the jammer's signal amplitude will be the most challenging. Thus, a more sophisticated method of deriving this estimate is required. It is desirable to use in-band signals to determine the jammer's signal amplitude; however, it may be possible to use a jammer's signal amplitude outside of the user's frequency band, but close to it. That is, a jammer's signal level just outside the user's frequency band might be used to estimate, or validate, the variation in the jammer's signal amplitude. This is especially true for wide-band jammers with a near-constant modulation envelope.

As with all adaptive AJ processors (temporal, spatial, and polarization), the undesired signals must be identified, or accurately estimated, in order to suppress them. The APNP studied in this Program partially identifies undesired signals by measuring the signal received at the user's cross-polarization port. When the user's polarization is know, only $|E_{jx}|$, that component of the jammer's signal that is cross-polarized to the user's signal, is received at this port. Recall that if the magnitude of the jammer's signal is known, θ_j (one of the jammer's signal polarization angles) can be determined by using $|E_{jx}|$. The APN described in this Study can use historical data to estimate the magnitude of the jammer's signal.

VII. Summary

This Study determines the probability of error in detecting QPSK-modulated signals in the presence of a jammer. It was shown in Figure 11a that, for a worst-case jammer signal polarization, estimating the jammer's amplitude within 2 dB may result in a probability of bit error, P_e, as large as 0.27. Assuming the jammer's polarization is varied over all possible polarizations, the probability of a bit error is about 0.15. The P_e is dependent on the jammer's polarization distribution—it can be as large as 0.27 or approach zero. The error analysis clearly indicates that using APN will reduce the BER below that obtained if APN is not used, except for those cases when the jammer's signal is nearly cross-polarized with the user's signal. In those cases, P_e with APN is less than ≈ 0.1.

The APN simulator indicates that, with a constant amplitude jammer signal, the APN can immediately determine the received jammer's signal amplitude and lock onto its signal polarization. As a result, there is at most one bit error at the onset of jamming and no errors in all the remaining bits transmitted. Up to 100 bits were transmitted with at least 99 received correctly. The jammer's in-band signal amplitude was equal to the user's signal amplitude. The user was communicating at 2400 bps and the jammer was varying its polarization such that its spectrum was spread over more than 3000 Hz. In other words, the jammer's polarization angles were varied through 2π radians at up to $2\pi 4000$ radians per second. Similar results were obtained with the jammer's amplitude and polarization varying. These are given in Table I. They indicate that APN does work and can be a useful AJ countermeasure.

The Study indicates that the algorithm can be, and should be, improved by using historical data to estimate the jammer's signal amplitude. It further indicates that the simulator can be improved by using more chips (of a transmitted bit) to determine the phase of the transmitted signal. This

would enable a larger variation in the jammer's signal amplitude. The Study does show that the basic algorithm has significant capability in suppressing jammer signals.

Examination of the principal equation for calculating the detected phase of the transmitted bit (see Equation (3)) shows that, as the jammer's signal amplitude increases above the user's signal amplitude, the accuracy required in estimating the jammer's signal amplitude decreases. The converse is true. Accuracy in estimating the jammer's signal amplitude determines the amount that this signal is suppressed. Thus, APN appears to perform best as better performance is required.

VIII. Recommendations

This Study has accomplished a great deal in demonstrating that APN can be useful as an AJ countermeasure. The next steps in its development should include developing a test bed that will include a QPSK transmitter and a pair of cooperative receivers—one with a horizontally polarized (HL) antenna and one with a vertically polarized (VL) antenna. A second transmitter should be used to radiate noise in the communication band via a pair of HL and VL antennas to simulate a jammer radiating a randomly polarized signal. Appropriately located "hooks" should be included in the receivers so that these signals can be simultaneously processed by an APNP. The comparable BER could be measured and a truly operational APN processor can be evaluated.

It is also advisable to carry-out the design of a COMSAT payload based on APN to accurately determine the cost and viability of such a device. In order to make this as economical as possible, the APN should be designed to operate at 2.4 kbps at either UHF or SHF so that its design would be readily transferable to an existing MILSATCOM satellite.

It may also be of interest to use APN in ground terminals to reduce self-jamming and incidental jamming effects. For example, a UHF terminal normally operates with a circularly polarized antenna. It is subject to accidental downlink jamming due to the enormous number of UHF communication terminals. In this case, the desired signal polarization and amplitude is very well known and the interfering signals are not designed to defeat the algorithm. Use of APN will permit significant suppression of the interfering signals and improve polarization match to the received downlink signal. It would require that each user's terminal have a dual-polarized antenna. It is likely that the cost of modifying a terminal will justify the improved operational capability.

IX. Acknowledgments

Many people were helpful in contributing to the acceptance of APN as a viable AJ countermeasure. It would be wrong to attempt to mention them all here out of fear that some would be omitted. However, Mr. Robert Cook deserves special mention because he demonstrated a sincere interest in its development and provided the support necessary to carry-out this Study. It is also true that the concept of using polarization to suppress jamming signals was first suggested to the principal author of this Report by Dr. Walter E. Morrow, Director of the Massachusetts Institute of Technology's Lincoln Laboratory.

Bit Error Probability

Jammer Amplitude Estimate Error: ±2 dB
User Amplitude Estimate Error: ±2dB
User Polarization Error: $\pm\pi/8$

Reference S/J=0 dB

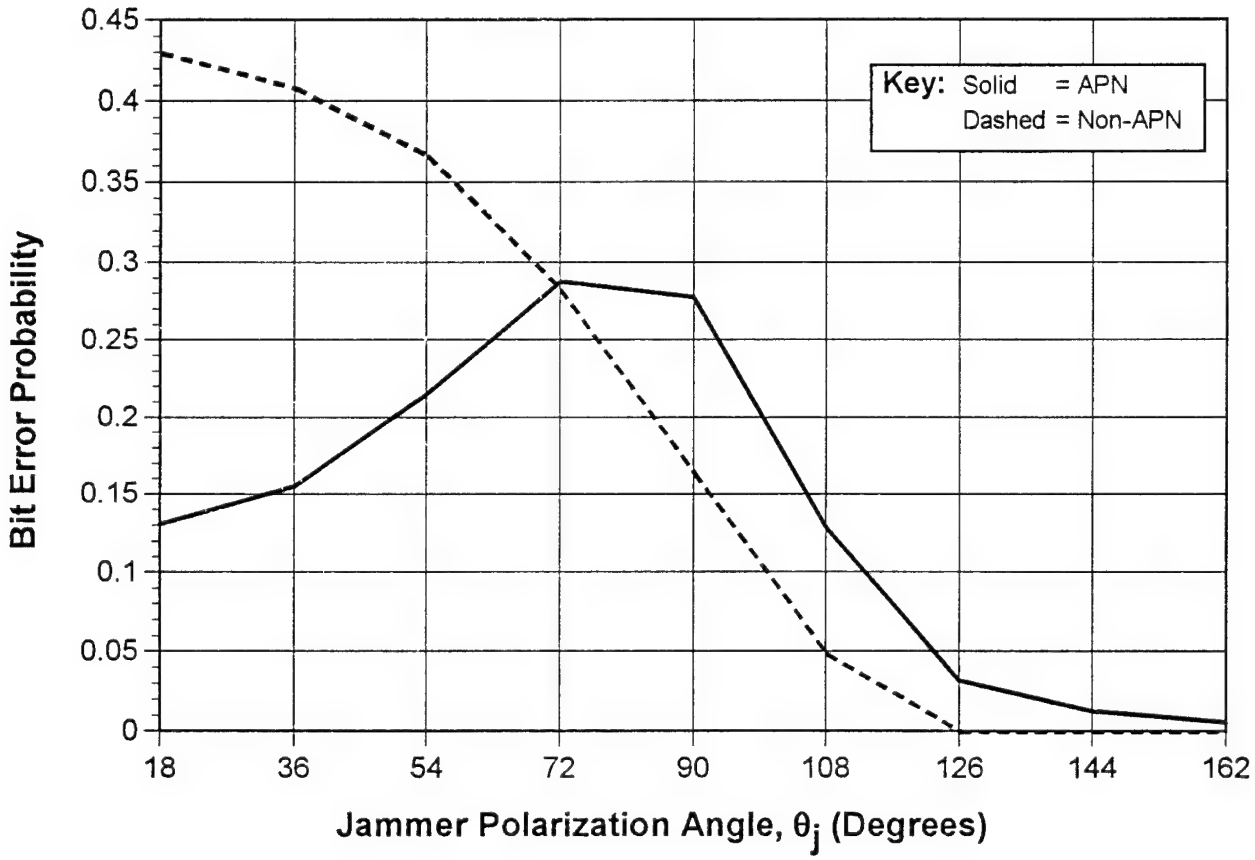

NOTE: For each point, the second jammer polarization angle, ϕ_j, and the relative phase between jammer and user signals, ζ, were varied over 360° in 20° increments.

Figure 1 – Overall Probability of Error

All Wave Polarizations Can Be Represented By A Poincarre Sphere:

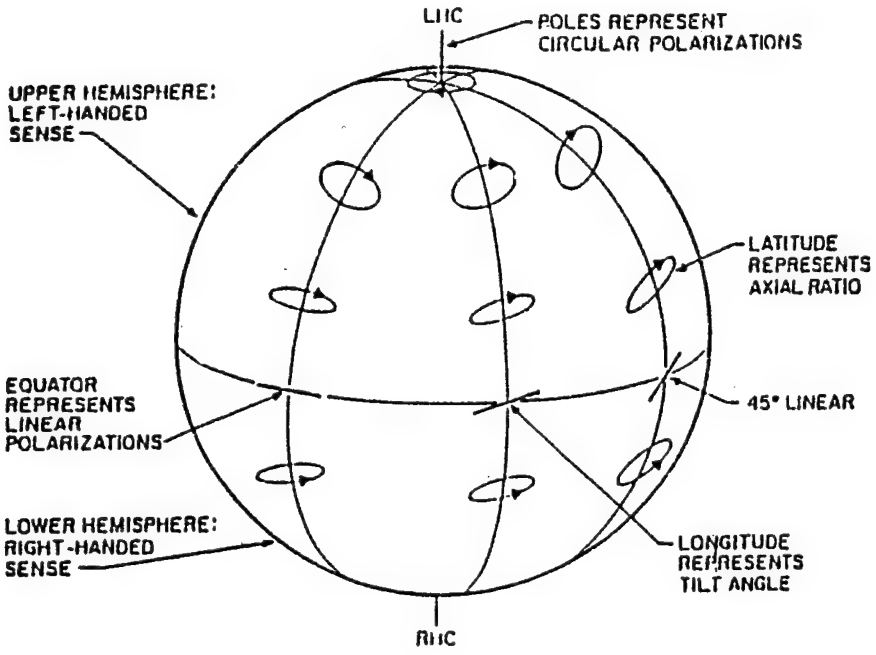

Figure 2 – Poincarre Polarization Sphere

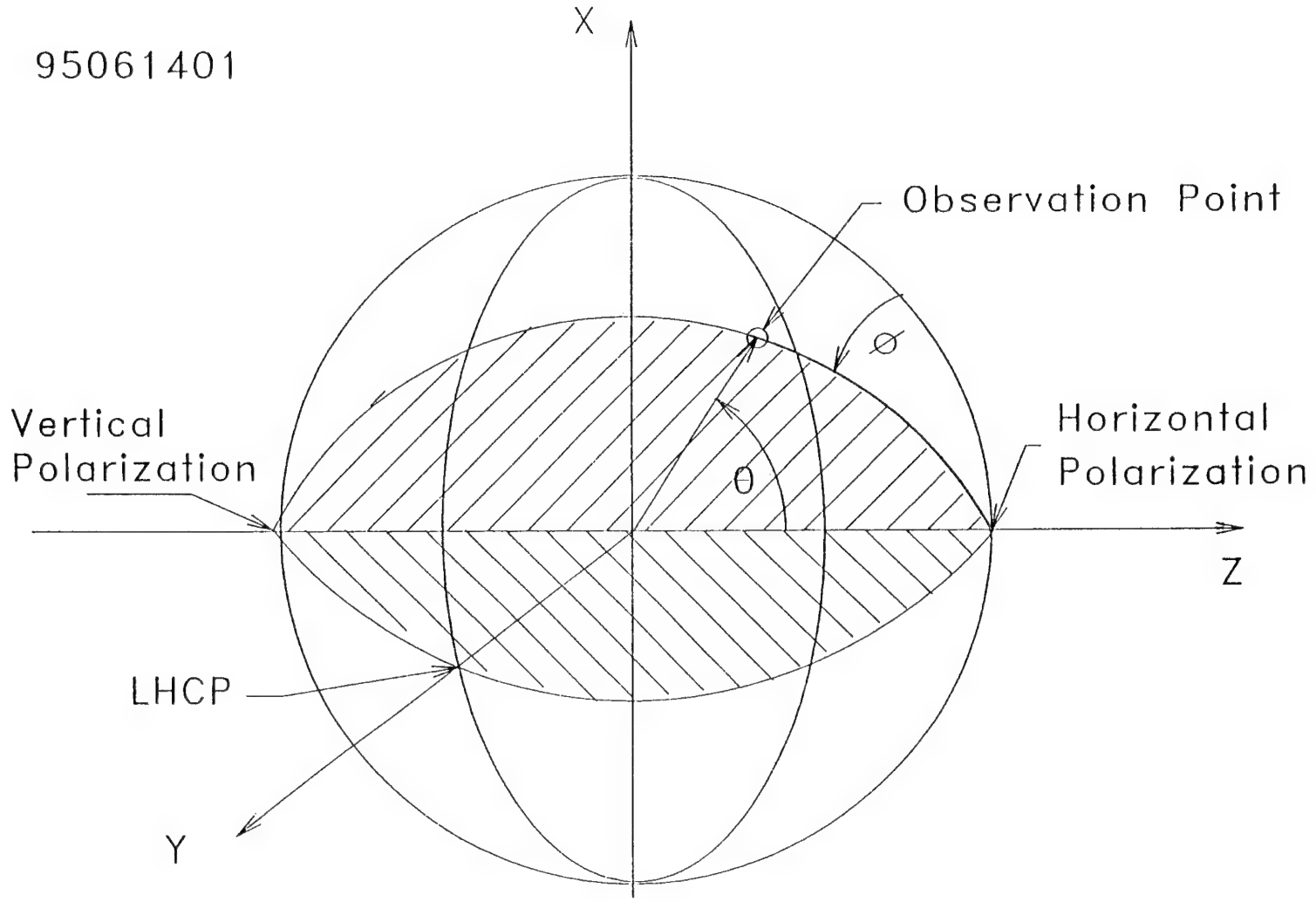

Modified Poincarre Polarization Sphere
And Coordinate Sytem

Figure 3 – Poincarre Polarization Sphere with Polarizations Shown

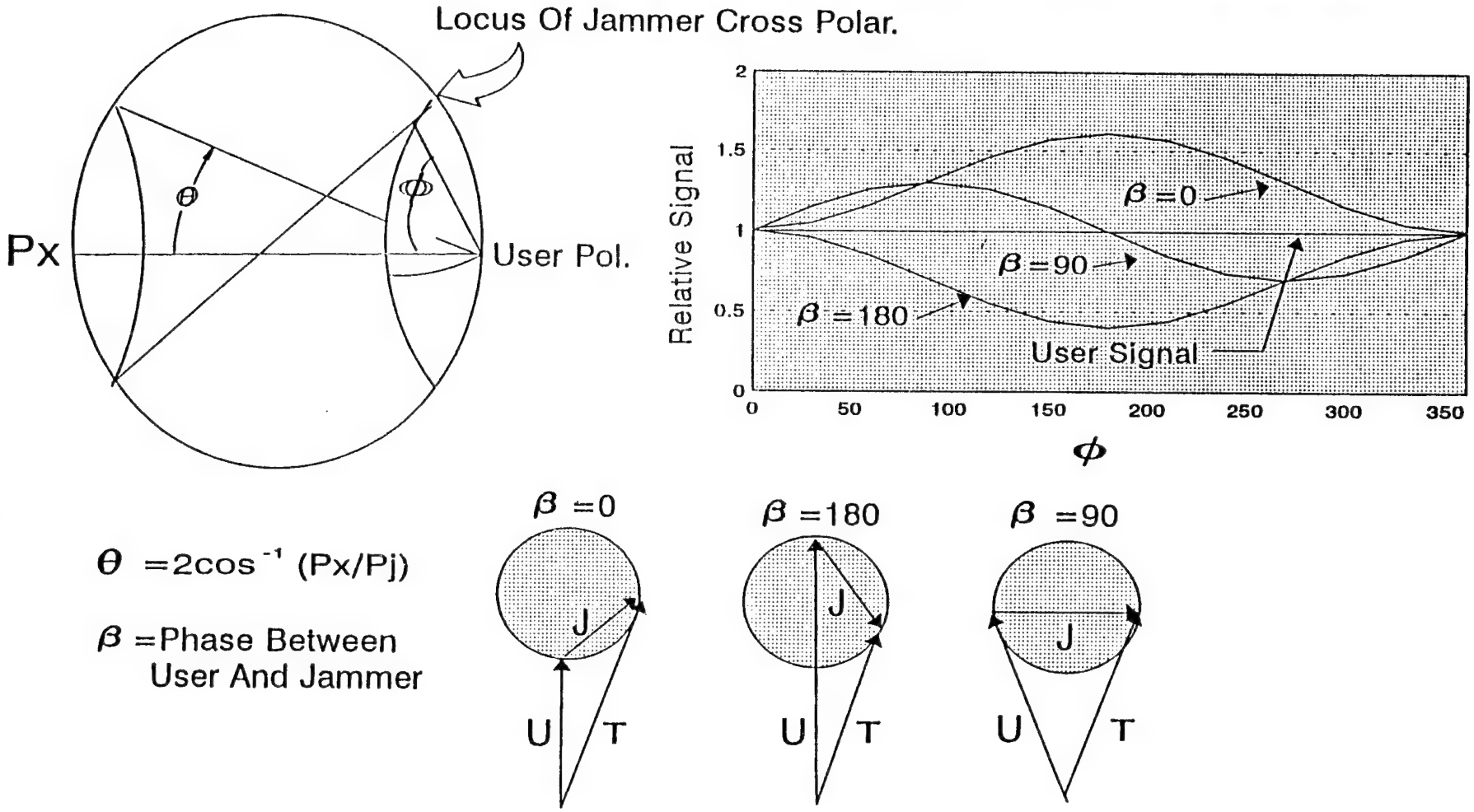

$\theta = 2\cos^{-1}(Px/Pj)$

β =Phase Between User And Jammer

Figure 4 – Jammer Cross-Polarization Location

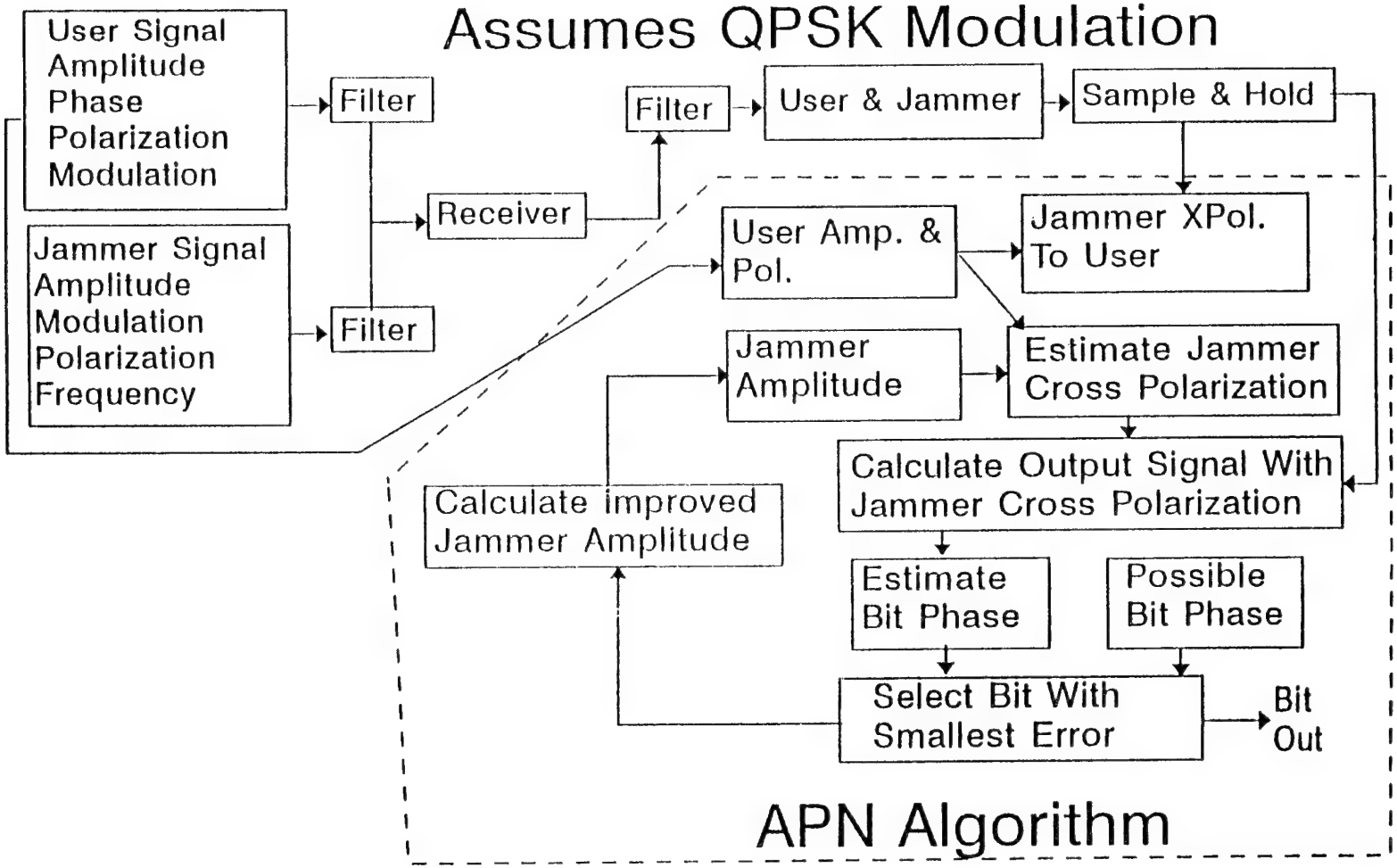

Figure 5 – APP Block Diagram

Bit Error Sensitivity

APN Algorithm Enabled

Correct Jammer Amplitude
Reference S/J=0 dB

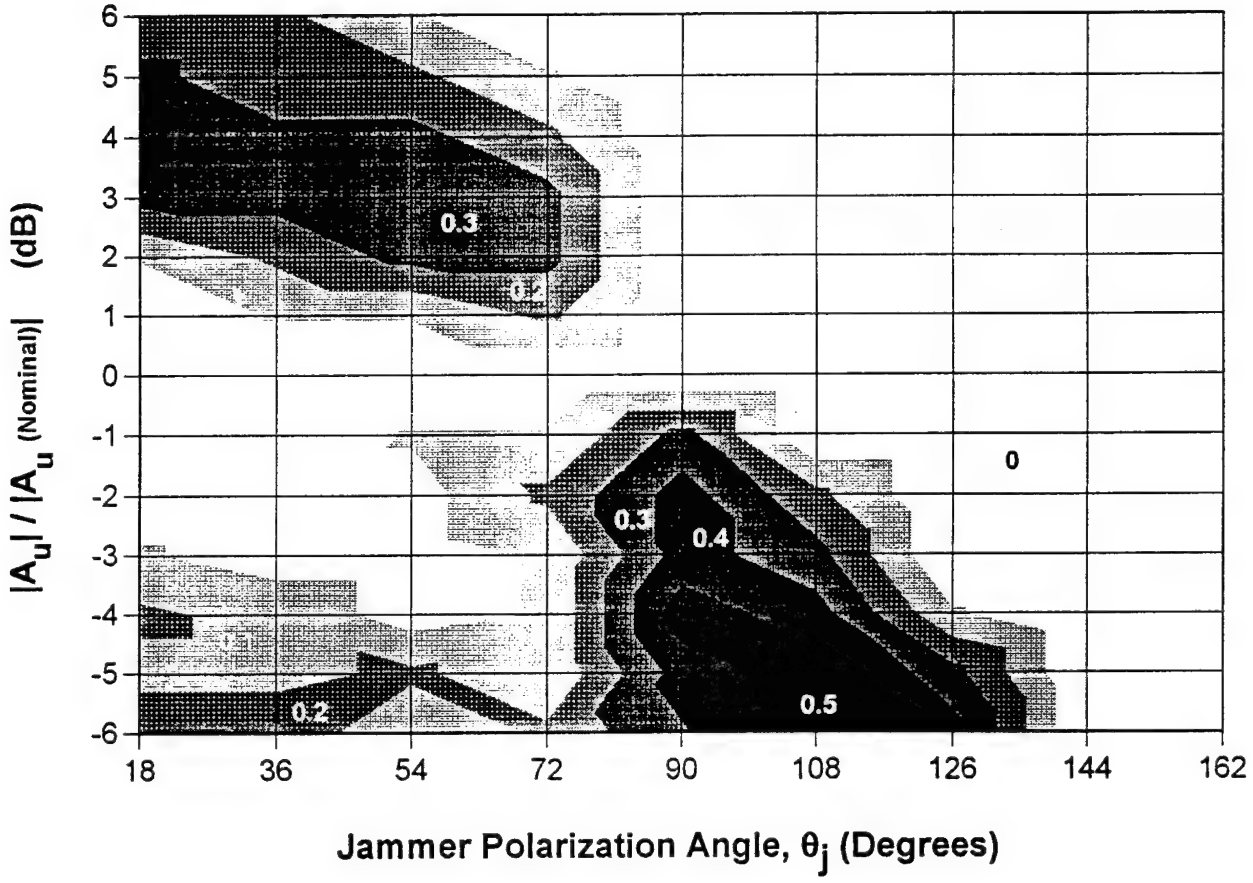

NOTE: For each point, the second jammer polarization angle, ϕ_j, and the relative phase between jammer and user signals, ζ, were varied over 360° in 20° increments.

Figure 6a – A100664

Bit Error Sensitivity

APN Algorithm Enabled

Correct User Amplitude and Polarization
Reference S/J=0 dB

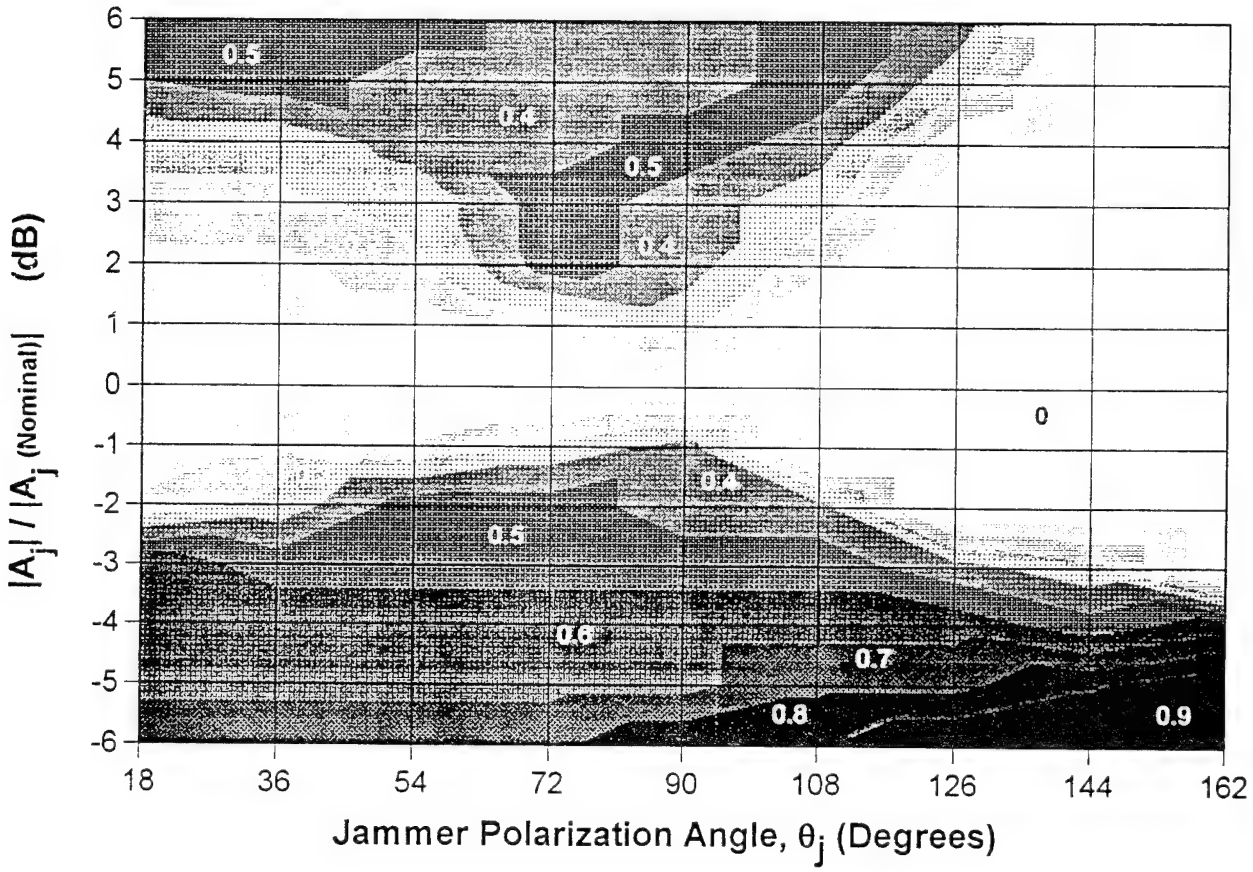

NOTE: For each point, the second jammer polarization angle, ϕ_j, and the relative phase between jammer and user signals, ζ, were varied over 360° in 20° increments.

Figure 6b – A200664

Bit Error Sensitivity

APN Algorithm Enabled

Correct User and Jammer Amplitude
Reference S/J=0 dB

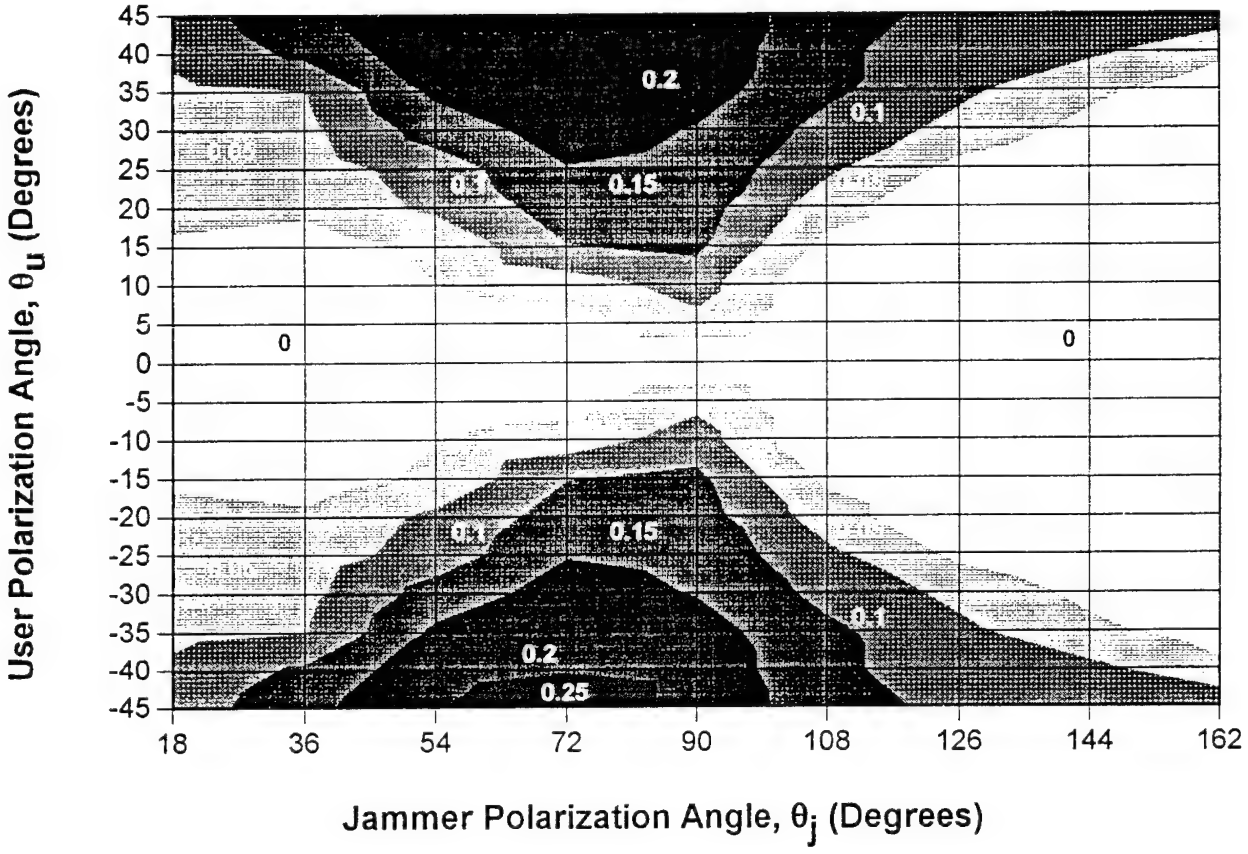

NOTE: For each point, the second jammer polarization angle, ϕ_j, and the relative phase between jammer and user signals, ζ, were varied over 360° in 20° increments.

Figure 6c – A300664

Bit Error Sensitivity

APN Algorithm Enabled

Correct Jammer Amplitude
Reference S/J=3 dB

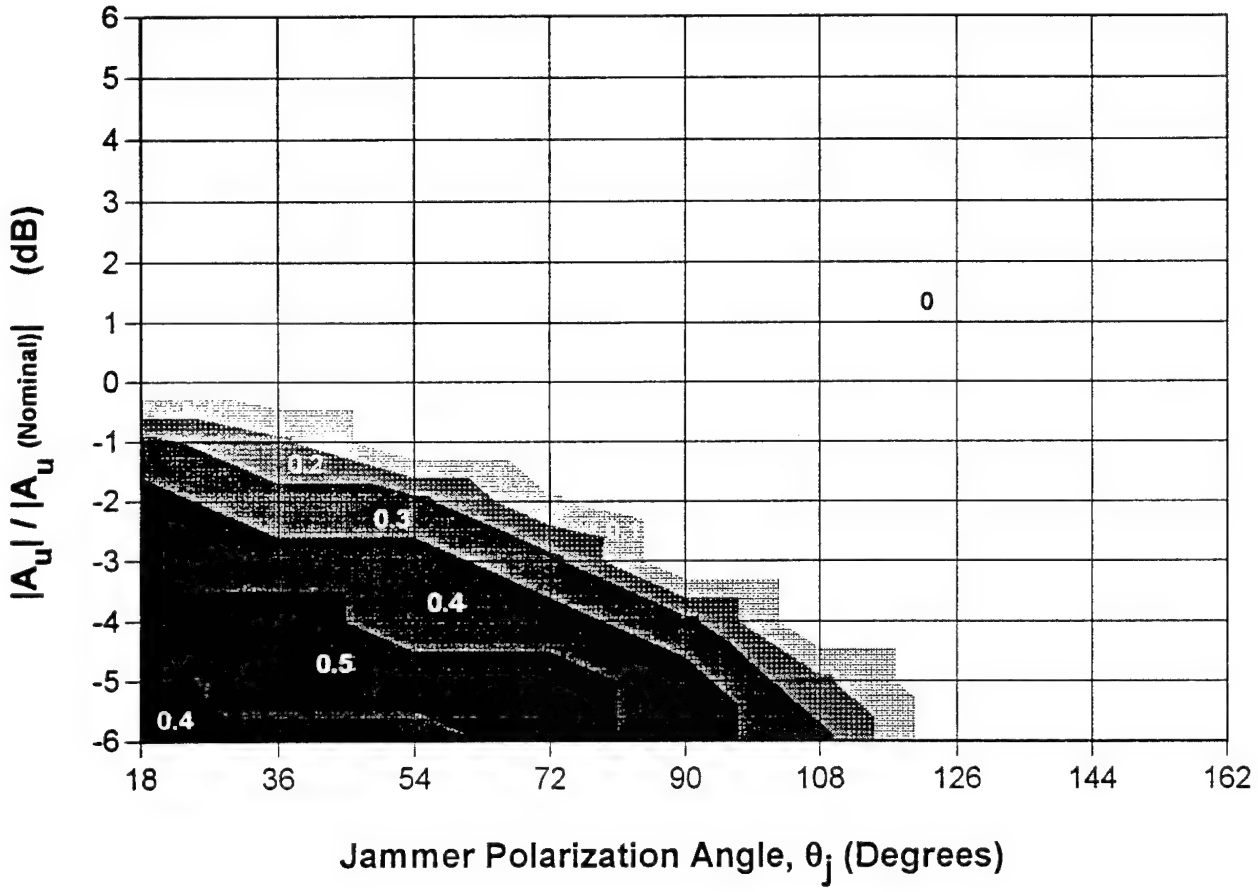

NOTE: For each point, the second jammer polarization angle, ϕ_j, and the relative phase between jammer and user signals, ζ, were varied over 360° in 20° increments.

Figure 7a – A103664

Bit Error Sensitivity

APN Algorithm Enabled

Correct User Amplitude and Polarization
Reference S/J=3 dB

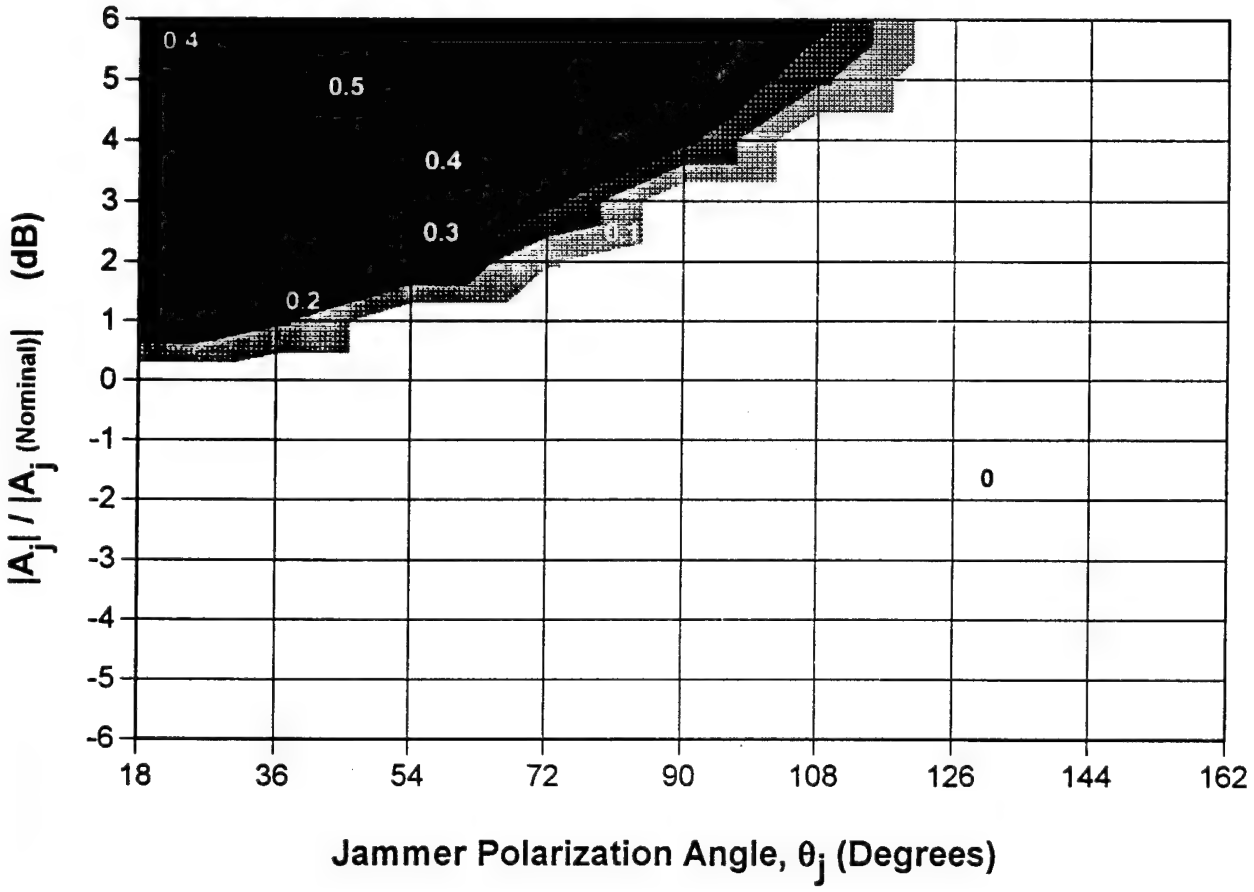

NOTE: For each point, the second jammer polarization angle, ϕ_j, and the relative phase between jammer and user signals, ζ, were varied over 360° in 20° increments.

Figure 7b – A203664

Bit Error Sensitivity

APN Algorithm Enabled

Correct User and Jammer Amplitude
Reference S/J=3 dB

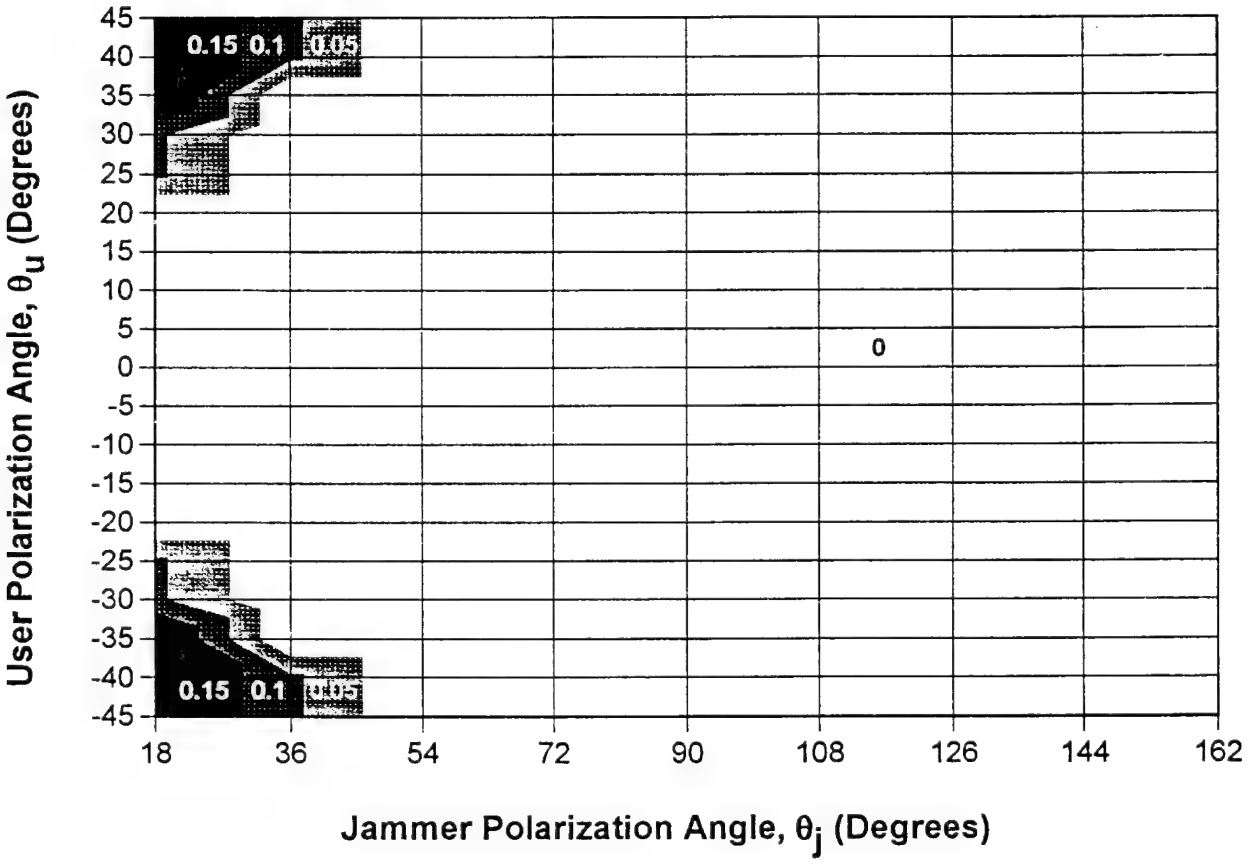

NOTE: For each point, the second jammer polarization angle, ϕ_j, and the relative phase between jammer and user signals, ζ, were varied over 360° in 20° increments.

Figure 7c – A303664

Bit Error Sensitivity

APN Algorithm Disabled

Correct Jammer Amplitude

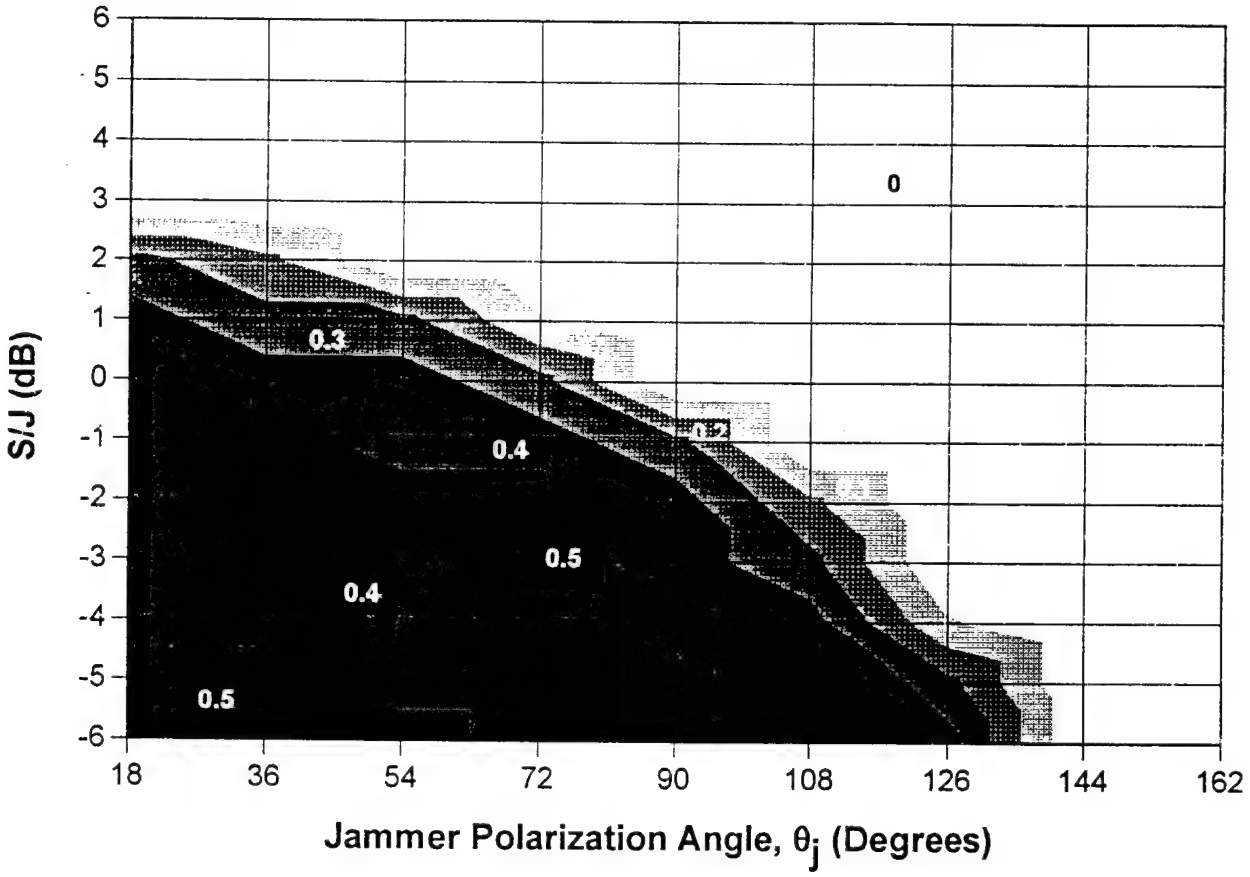

NOTE: For each point, the second jammer polarization angle, ϕ_j, and the relative phase between jammer and user signals, ζ, were varied over 360° in 20° increments.

Figure 8a – N100664

Bit Error Sensitivity

APN Algorithm Disabled

Correct User Amplitude and Polarization

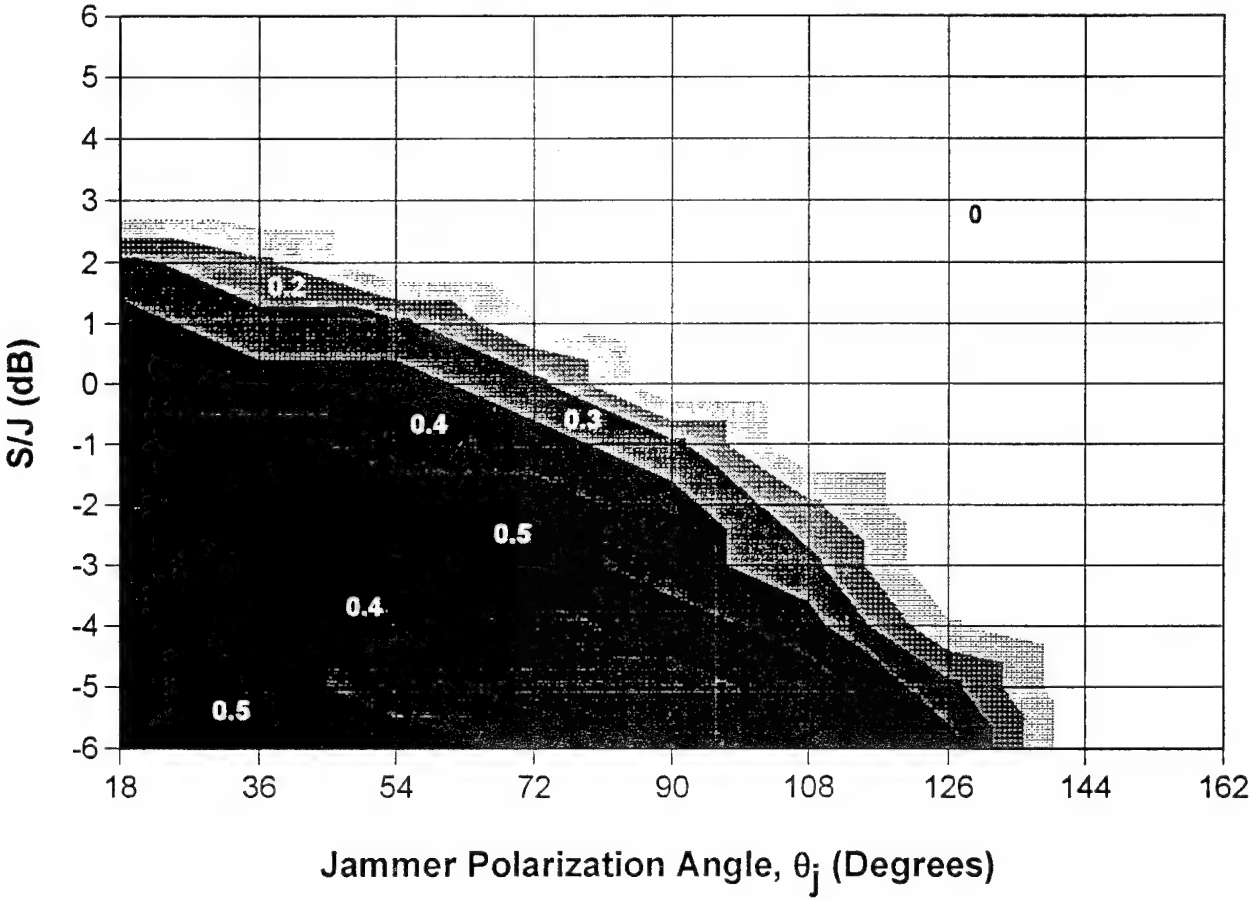

NOTE: For each point, the second jammer polarization angle, ϕ_j, and the relative phase between jammer and user signals, ζ, were varied over 360° in 20° increments.

Figure 8b – N200664

Bit Error Sensitivity

APN Algorithm Disabled

Correct User and Jammer Amplitude
Reference S/J=0 dB

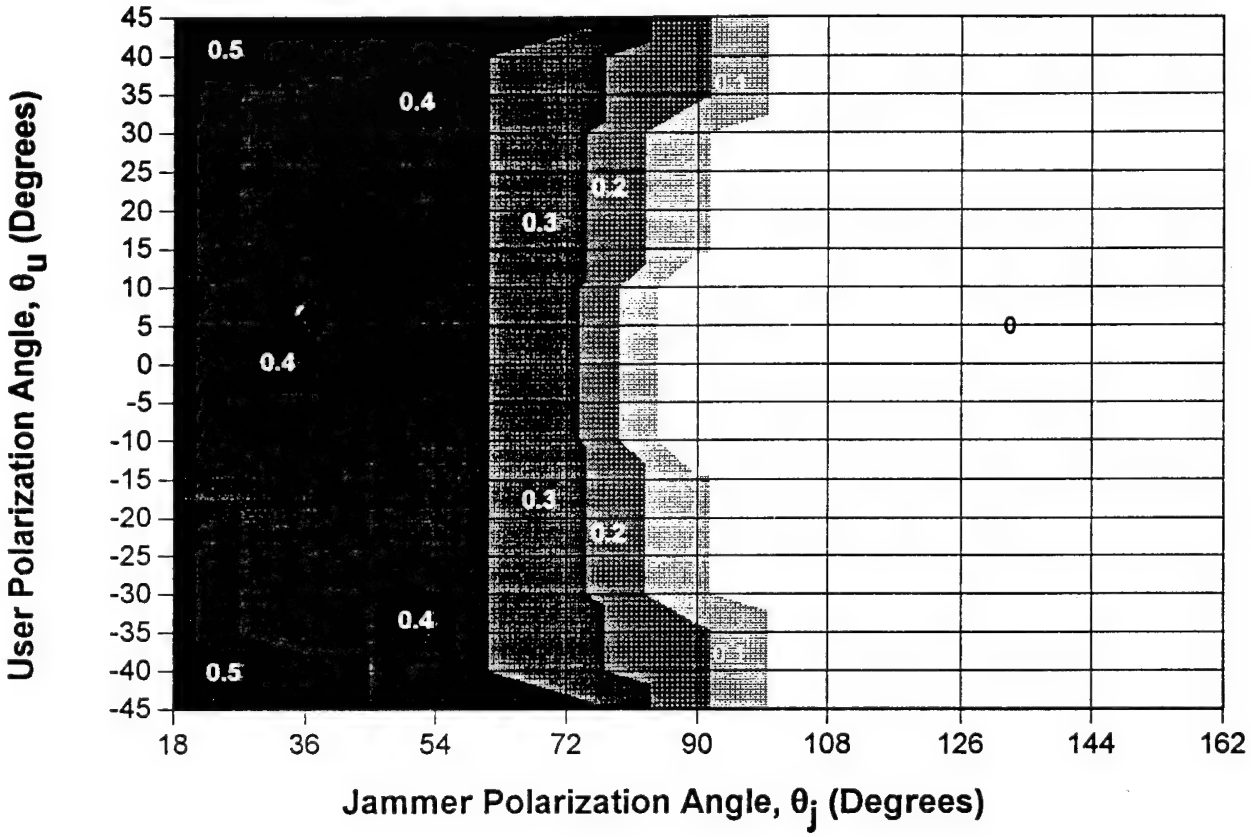

NOTE: For each point, the second jammer polarization angle, ϕ_j, and the relative phase between jammer and user signals, ζ, were varied over 360° in 20° increments.

Figure 8c – N300664

Bit Error Sensitivity

APN Algorithm Disabled

Correct Jammer Amplitude

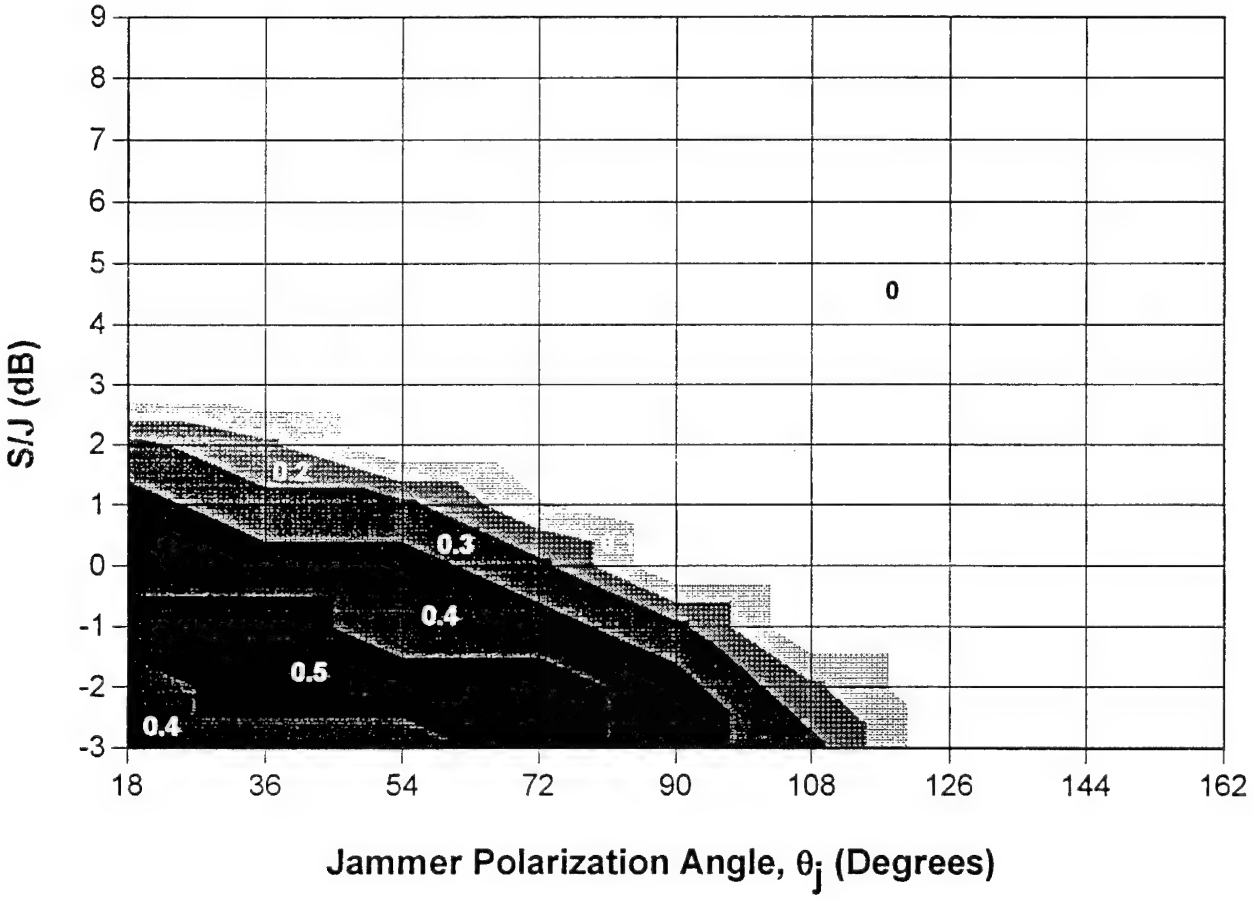

NOTE: For each point, the second jammer polarization angle, ϕ_j, and the relative phase between jammer and user signals, ζ, were varied over 360° in 20° increments.

Figure 9a – N103664

Bit Error Sensitivity

APN Algorithm Disabled

Correct User Amplitude and Polarization

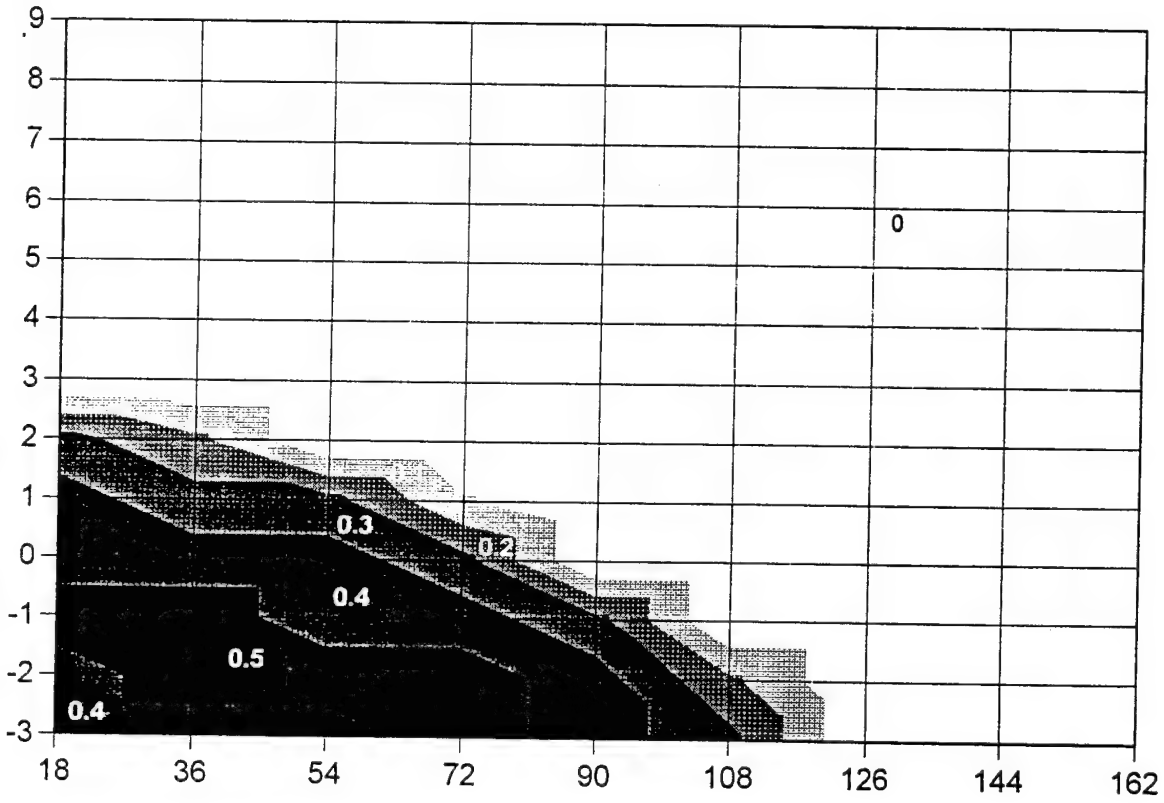

NOTE: For each point, the second jammer polarization angle, ϕ_j, and the relative phase between jammer and user signals, ζ, were varied over 360° in 20° increments.

Figure 9b – N203664

Bit Error Sensitivity

APN Algorithm Disabled

Correct User and Jammer Amplitude
Reference S/J=3 dB

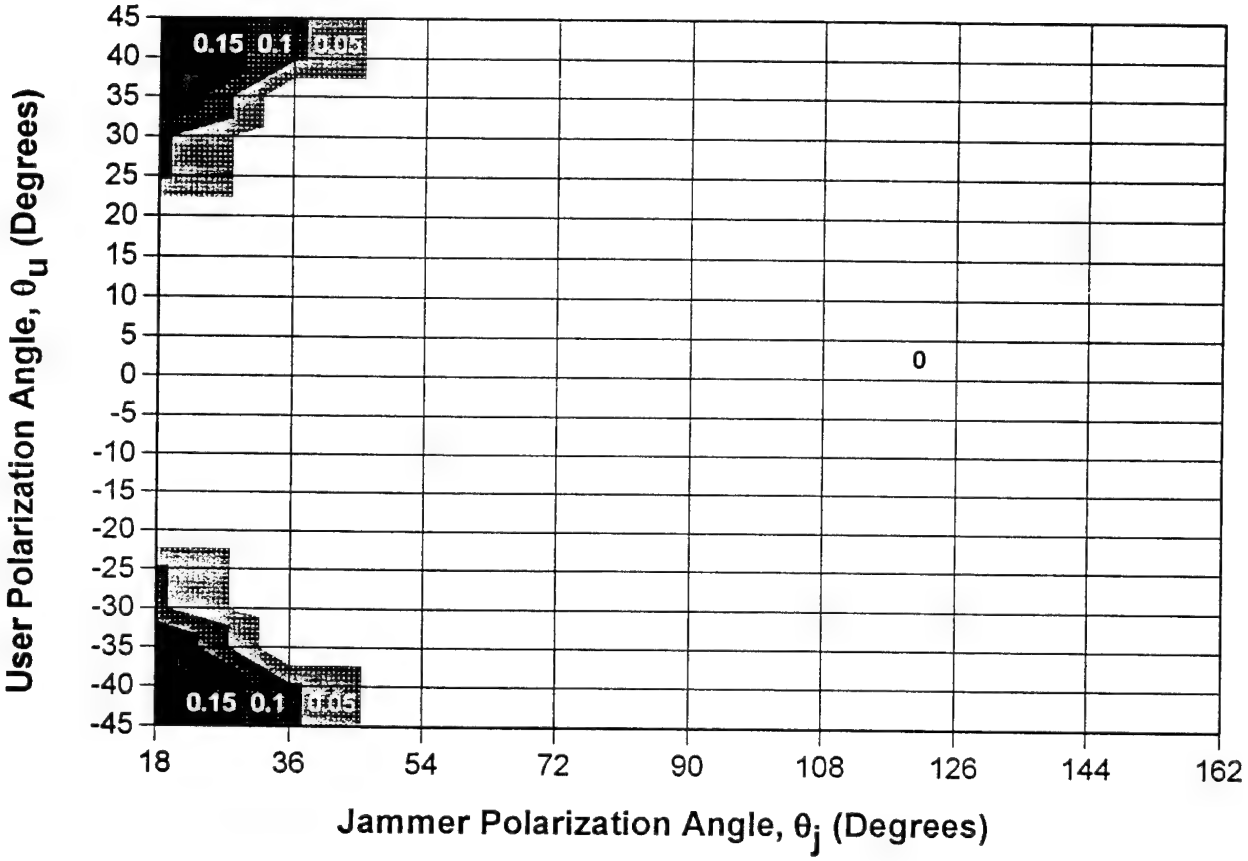

NOTE: For each point, the second jammer polarization angle, ϕ_j, and the relative phase between jammer and user signals, ζ, were varied over 360° in 20° increments.

Figure 9c – N303664

Probability Distribution
For Variation In
User's And Jammer's Amplitude, ±2 dB

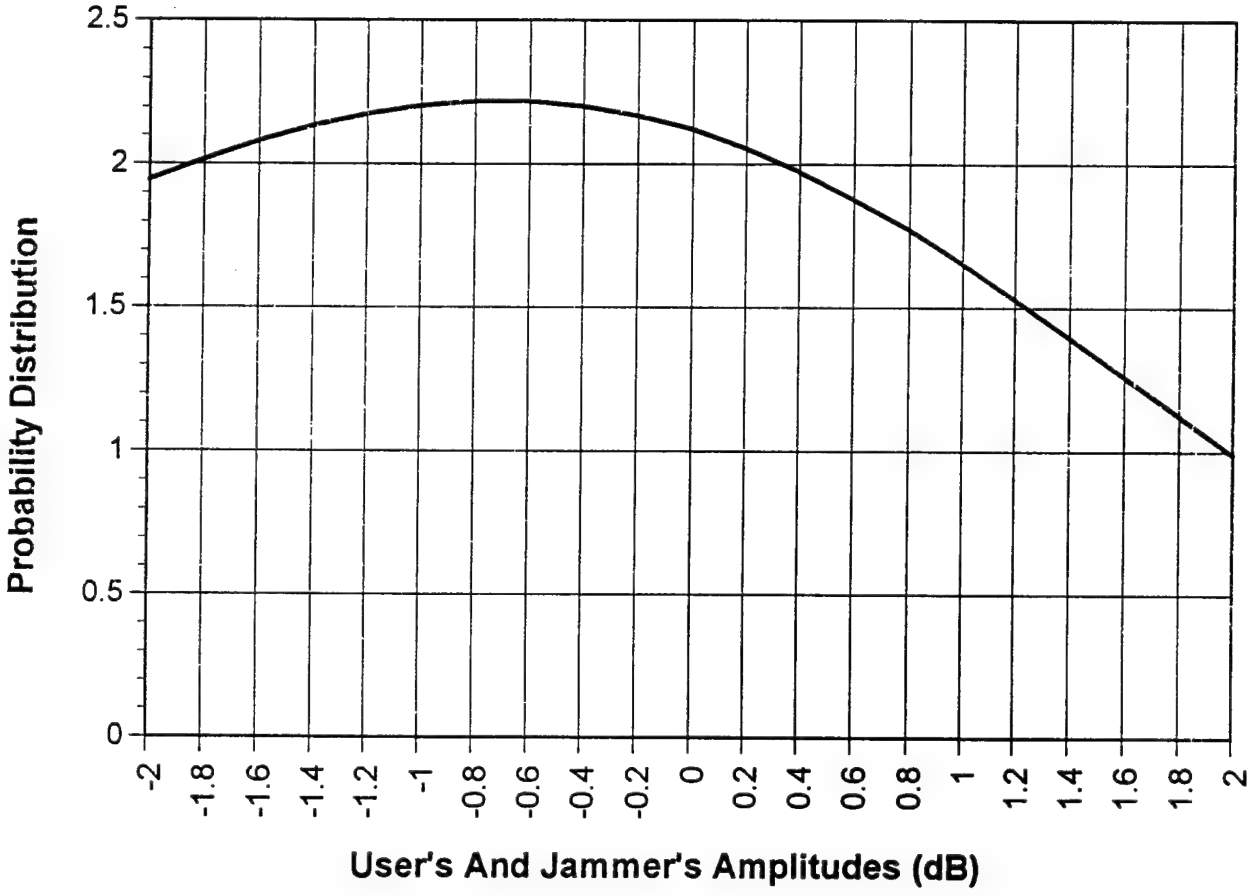

Figure 10a – Probability Distribution, User And Jammer Amplitudes

Probability Distribution
For Variation In
User's Polarization Angle, θ_u, $\pm\pi/8$

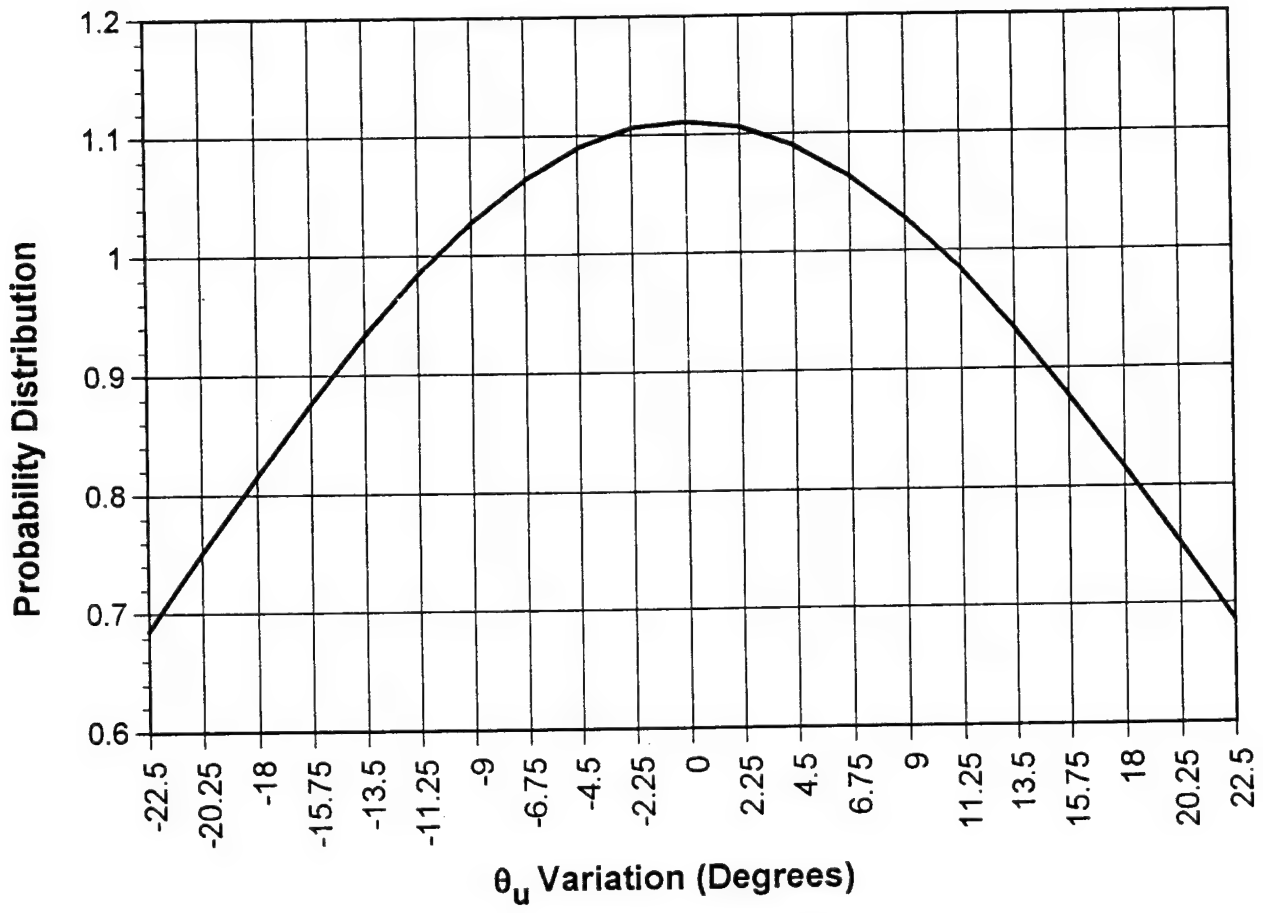

Figure 10b — Probability Distribution, θ_u Variation

Bit Error Probability

Jammer Amplitude Estimate Error: ±2 dB
User Amplitude Estimate Error: ±2dB
User Polarization Error: $\pm\pi/8$

Reference S/J=0 dB

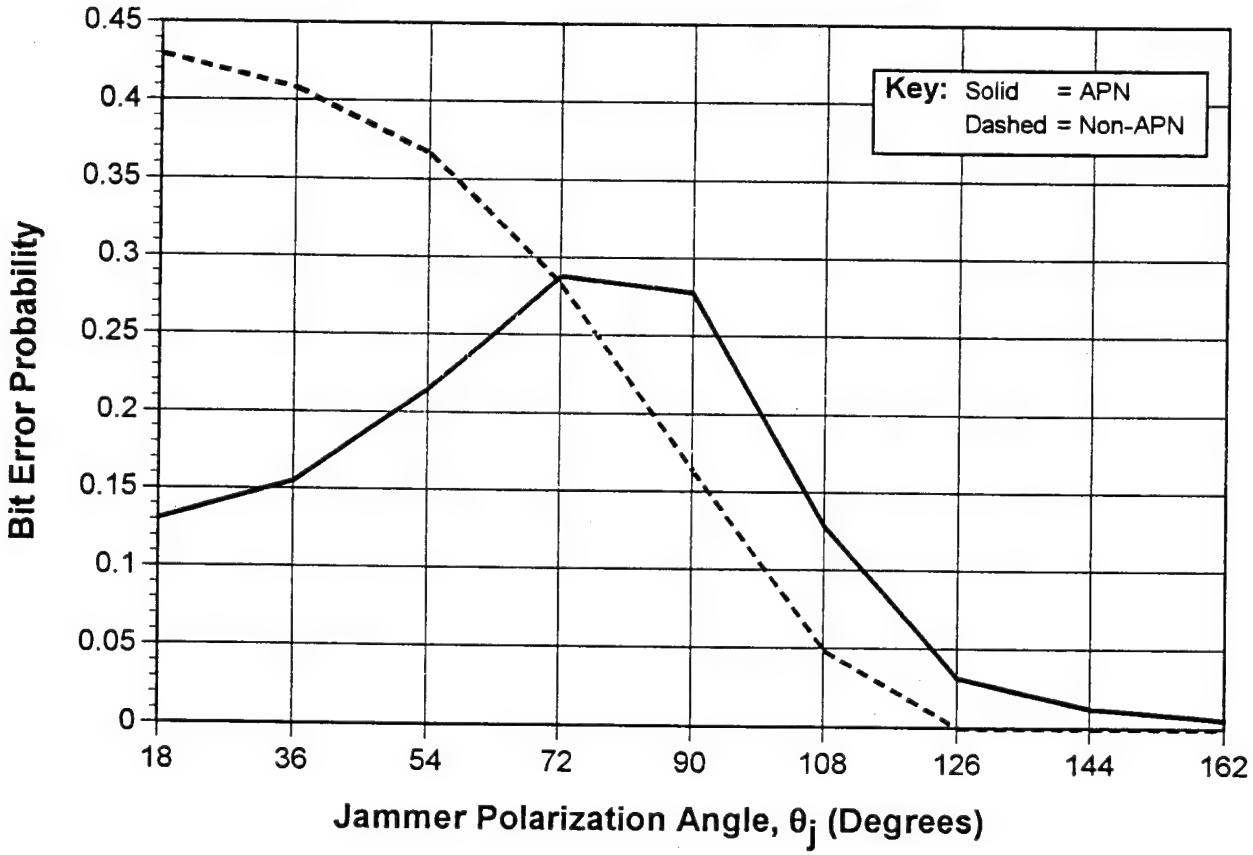

NOTE: For each point, the second jammer polarization angle, ϕ_j, and the relative phase between jammer and user signals, ζ, were varied over 360° in 20° increments.

Figure 11a – Overall Bit Error Probability, S/J = 0 dB

Bit Error Probability

User Amplitude Estimate Error: ±2dB
User Polarization Error: ±π/8

Reference S/J = -3 dB

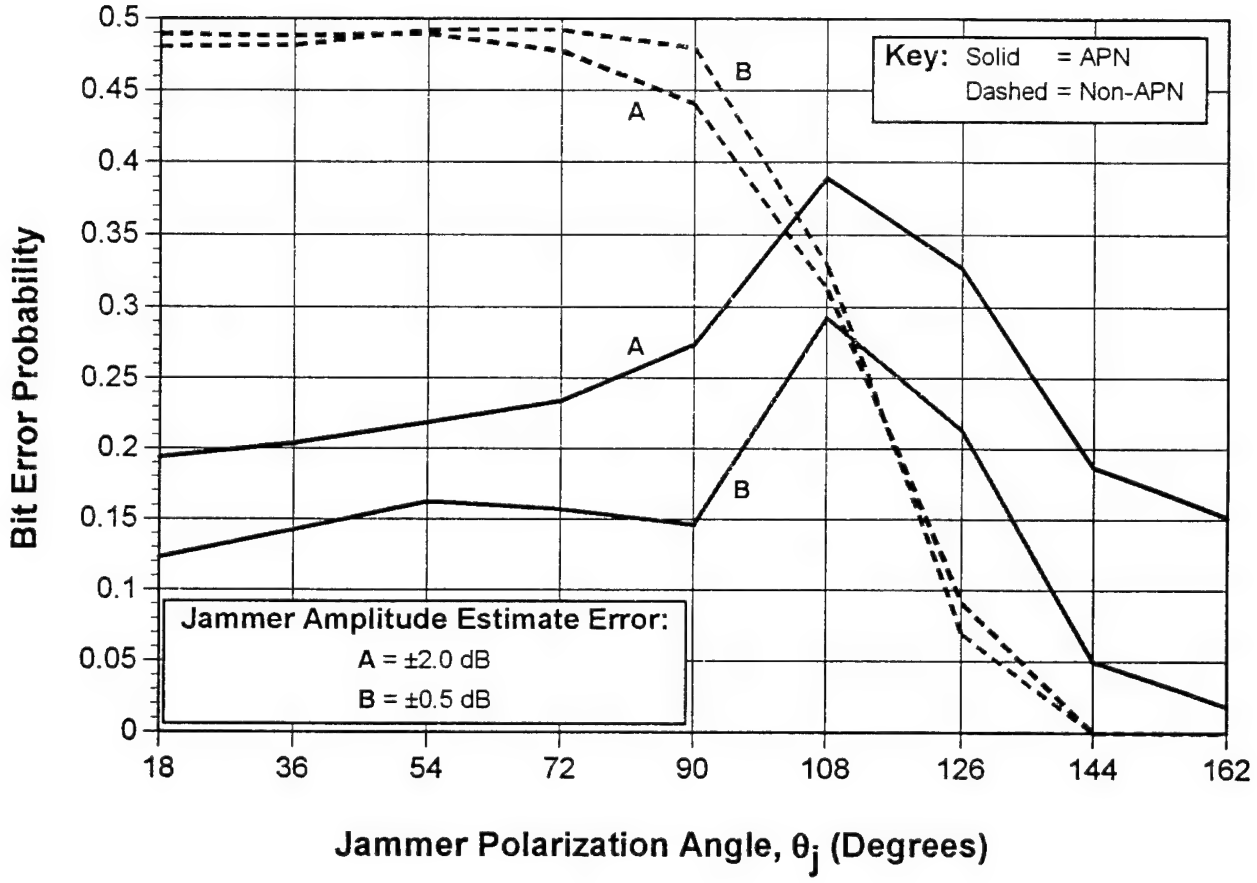

NOTE: For each point, the second jammer polarization angle, ϕ_j, and the relative phase between jammer and user signals, ζ, were varied over 360° in 20° increments.

Figure 11b – Overall Bit Error Probability, S/J = -3 dB

APN Block Diagram

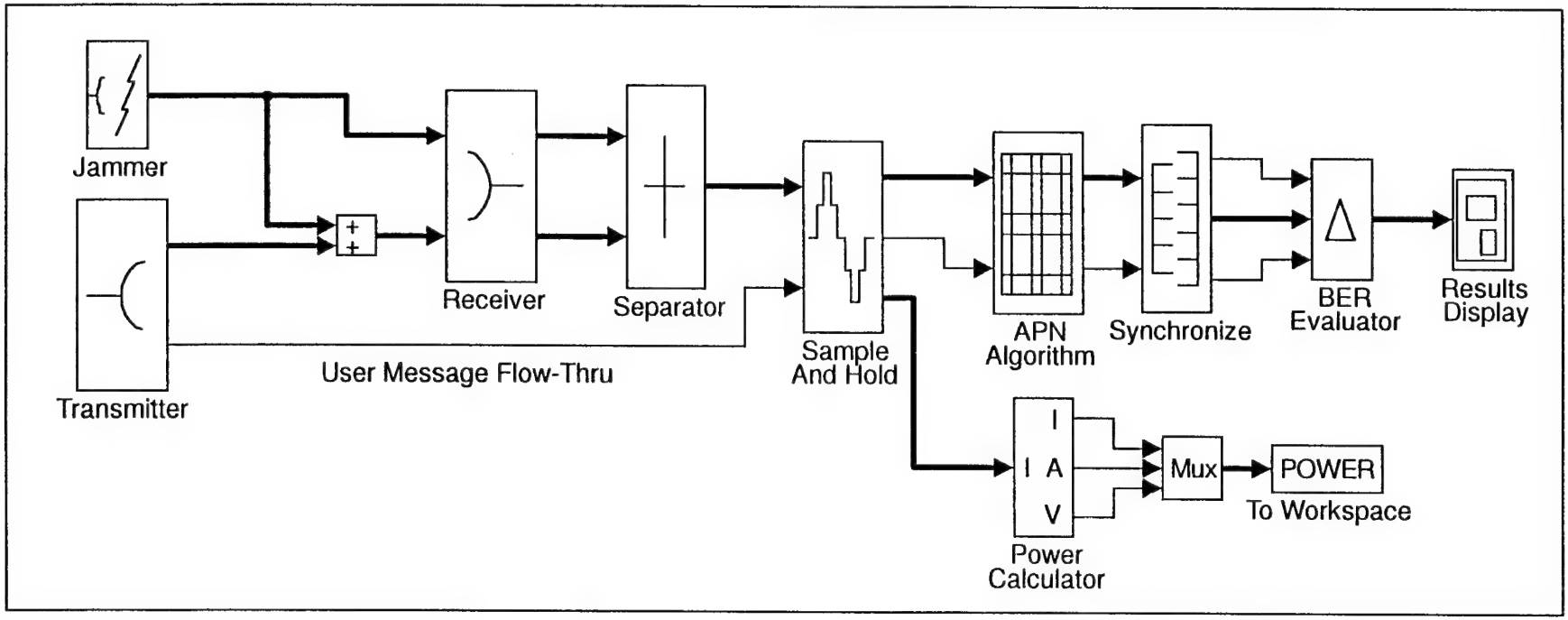

Figure 12 – Simulator Block Diagram, Root

Transmitter

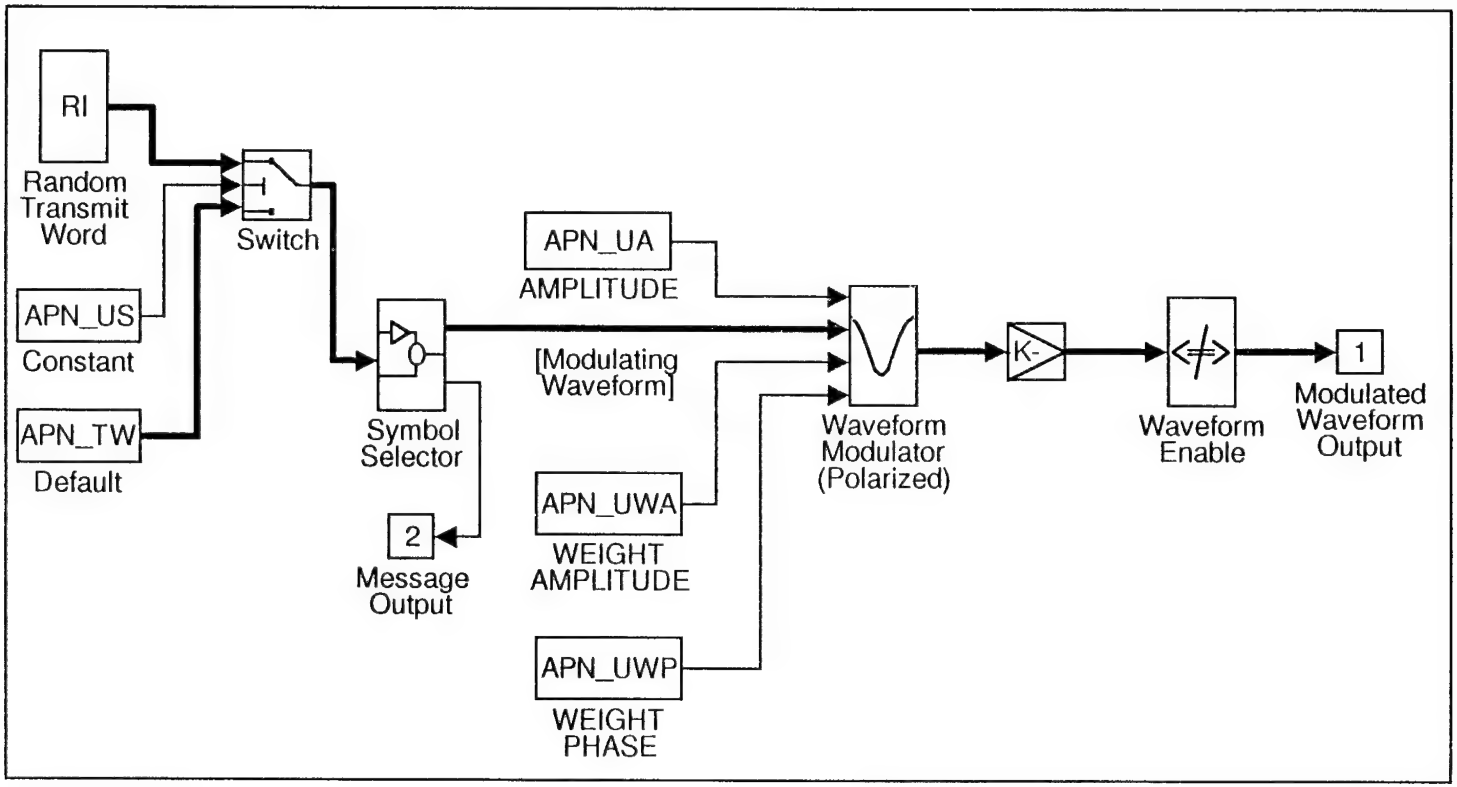

The Transmitter outputs a QPSK-modulated horizontally and vertically polarized signal. The modulation comes from a four-bit message word which can either be randomly generated or specified as a input variable. The Symbol Selector is responsible for extracting the correct bit from the four-bit message word and converting it to a phase modulating signal. The Waveform Modulator takes this phase modulation and applies it to a polarized carrier. The polarization and amplitude of the output waveform can be controlled by input variables. The Waveform Enable is an ancillary function that allows the Transmitter to be turned on or off.

Figure 12a – Simulator Block Diagram, Transmitter Branch

Jammer

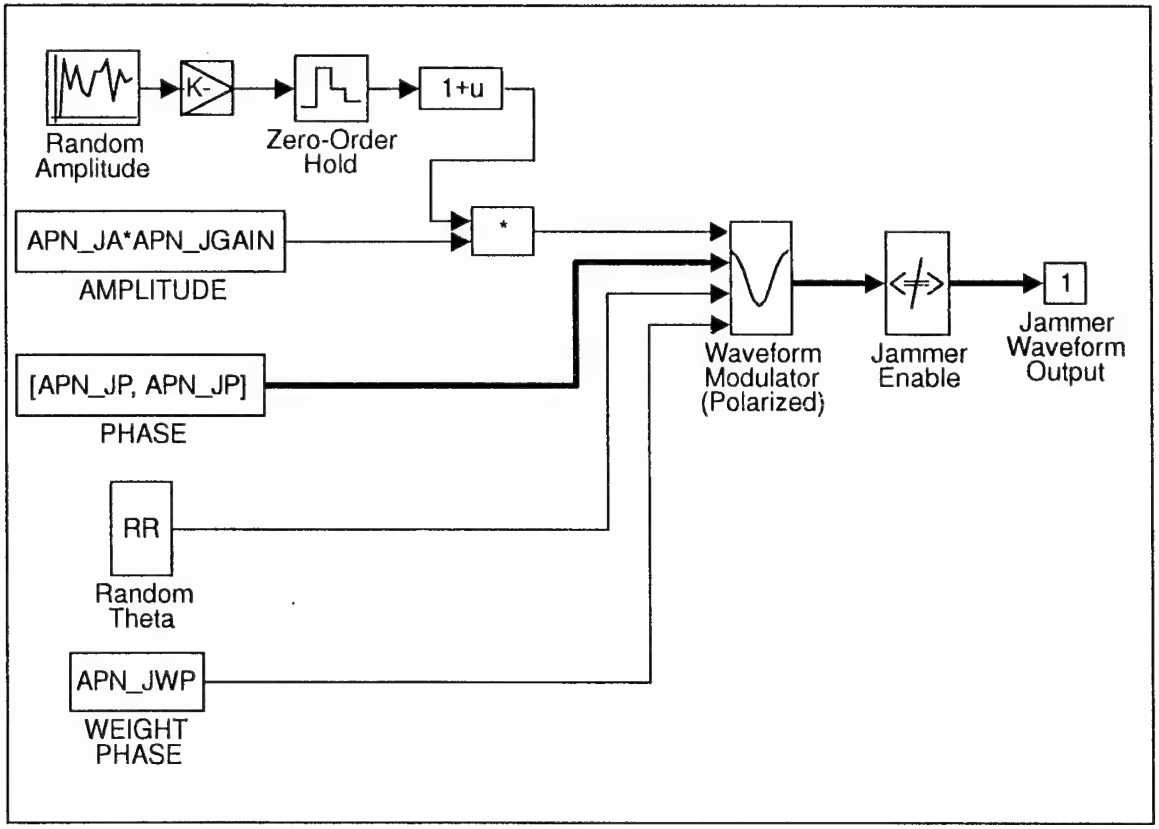

The Jammer outputs random amplitude and random polarization signals. The Jammer can be made to output other combinations of fixed / random signal amplitudes and polarizations. The Waveform Modulator outputs a fixed-phase, fixed or random amplitude, fixed or random polarization tone. The signal amplitude and polarization can be changed randomly, with variable bandwidth, by input variables. The Jammer Enable is an ancillary function that allows the Jammer to be turned on or off.

Figure 12b – Simulator Block Diagram, Jammer Branch

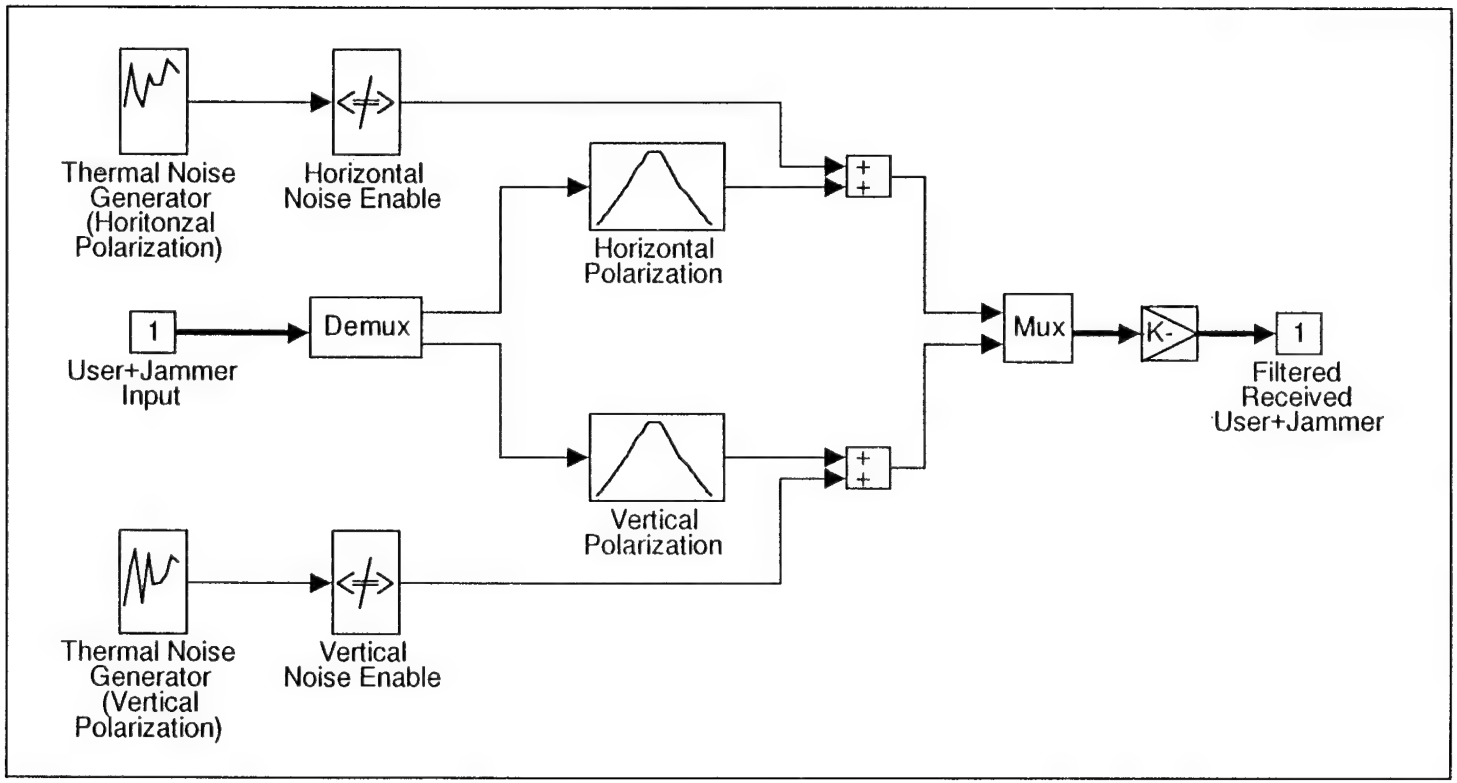

The Receiver filters the combined User's and Jammer's signals before being input to the Separator. A gain stage is provided, as well as models for Thermal Noise.

Figure 12c – Simulator Block Diagram, Receiver Branch

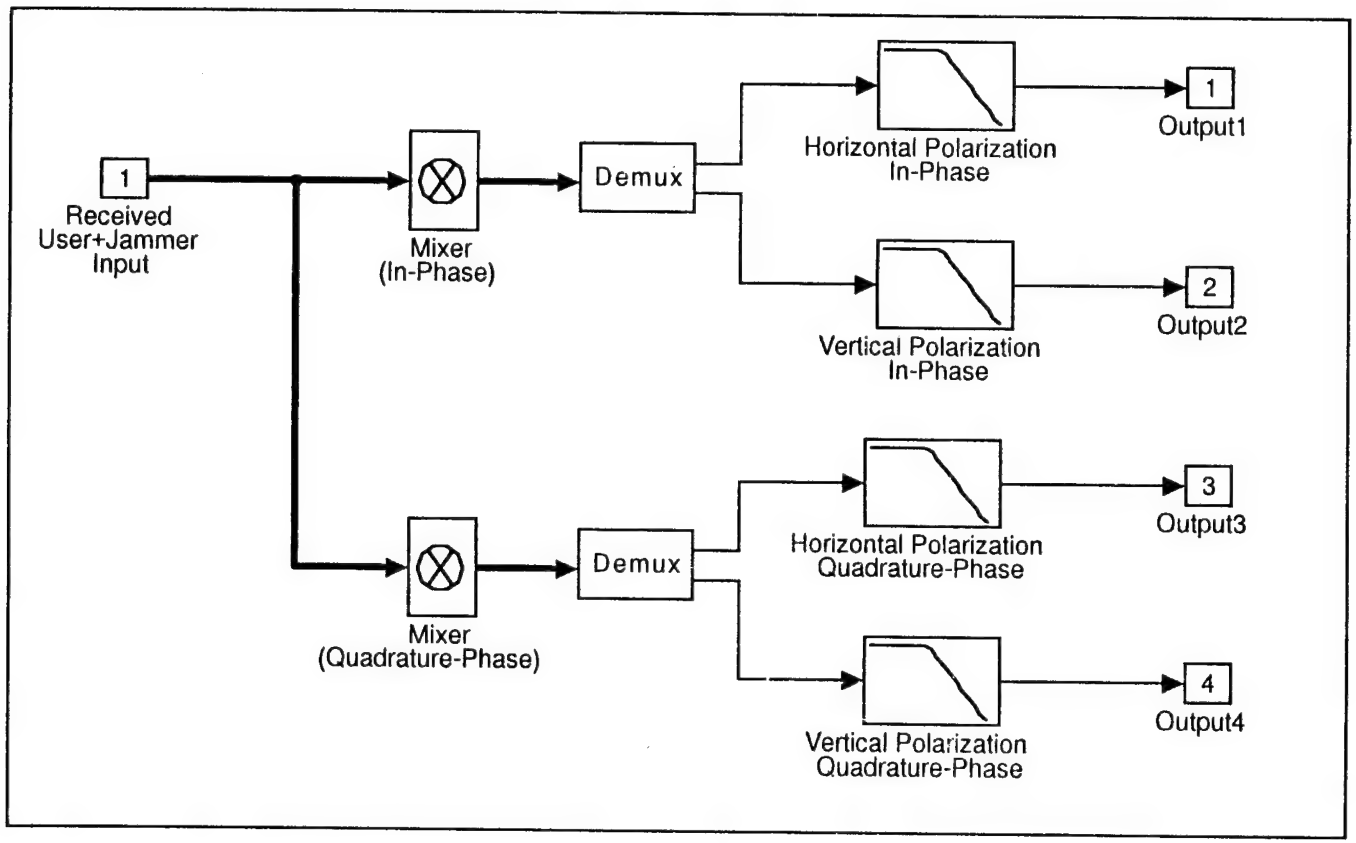

The Separator mixes (beats) the incoming RF signals by cosine and sine waveforms with the same frequency as the User and Jammer carriers to produce both Sum and Difference signals. The Sum signals give frequency components of twice the carrier frequency which are filtered to allow the Difference channel signals, now at baseband, to pass. Mixing by the cosine carrier results in in-phase signals; whereas mixing by the sine carrier results in quadrature-phase signals. The phasing of these I and Q signals relates to the transmitted QPSK message. These phases are input to the APN Algorithm, which then nulls the Jammer and detects the resulting message.

Figure 12d – Simulator Block Diagram, Separator Branch

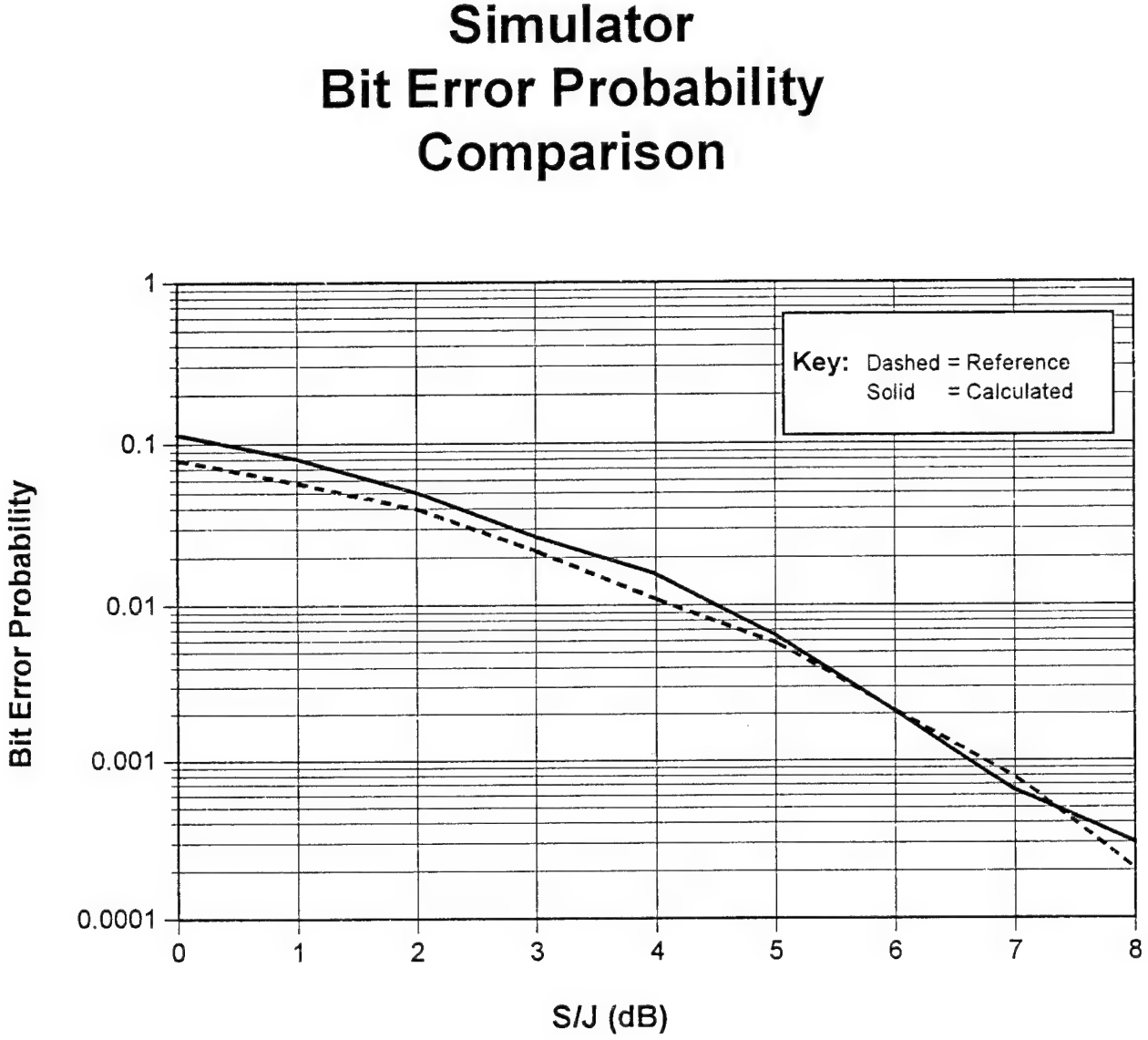

Figure 13 – Simulator Bit Error Probability Comparison with Published Chart

APN Algorithm Performance Improvement

Average User Power: 1.00 W, Variation in User Power: 0.07 W

100 Bits Transmitted, Algorithm Non-Damped

Ao (Random)	θ Type	θ Range	Fj (Hz)	Jammer Power (Watts) Average	Jammer Power (Watts) Variation	Bit Error Probability (Percent) Non-APN	Bit Error Probability (Percent) APN
0 V	Random	0–π	500	1.00	0.07	25	0
			1000	1.00	0.07	25	0
			2000	1.00	0.07	19	0
			4000	1.00	0.07	18	1
±50 mV	Random	0–π	500	1.00	0.10	25	5
			1000	0.99	0.11	25	9
			2000	0.99	0.12	19	7
			4000	1.00	0.12	17	10
	Fixed	π/4	500	1.00	0.10	55	8
			1000	0.99	0.11	51	7
			2000	0.99	0.12	51	20
			4000	1.00	0.12	52	40
±100 mV	Random	0–π	500	1.01	0.16	21	10
			1000	0.98	0.19	17	14
			2000	1.00	0.20	15	14
			4000	1.01	0.21	14	30
	Fixed	π/4	500	1.01	0.16	50	22
			1000	0.98	0.19	43	23
			2000	1.00	0.20	43	39
			4000	1.01	0.21	38	58
±200 mV	Random	0–π	500	1.04	0.30	24	26
			1000	0.99	0.35	14	52
			2000	1.02	0.38	15	53
			4000	1.04	0.39	15	53
	Fixed	π/4	500	1.04	0.30	46	33
			1000	0.99	0.35	33	46
			2000	1.02	0.38	39	59
			4000	1.04	0.39	35	57

Table I

Appendix A

Antenna Polarization Nulling Analysis

Dr. J.P. Mahon
LJR, Inc.
360 N. Sepulveda Blvd., Suite 2030
El Segundo CA 90245

May 11, 1995

Contents

1 Mapping From a General Polarization Vector to the Poincare Sphere

Let the two measured polarizations be denoted by horizontal and vertical and let the unit vectors for these polarizations be $\vec{1}_h$ and $\vec{1}_v$, respectively.

Now consider the Poincare sphere. Let the cartesian coordinates for a point on the sphere be (x, y, z) and let the spherical coordinates be $(1, \theta, \phi)$. Let the cartesian unit vectors be $\vec{1}_x$, $\vec{1}_y$ and $\vec{1}_z$.

The mapping from the polarizations to the sphere is not unique since the coordinate system of the sphere can be rotated without affecting the relative relationships of the mapping. In order to specify the mapping uniquely, two polarizations which are not cross-polarized must be mapped to the sphere. Let pure horizontal polarization map to $(x, y, z) = (0, 0, 1)$ and let in-phase, 45°-linear polarization map to $(x, y, z) = (1, 0, 0)$.

Consider the point on the sphere with spherical coordinates $(1, \theta, \phi)$. It corresponds to the polarization whose unit vector is given by $\vec{P}(\theta, \phi)$ where

$$\begin{aligned} \vec{P}(\theta, \phi) &= p_h \vec{1}_h + p_v \vec{1}_v \\ &= \cos\frac{\theta}{2}\vec{1}_h - e^{j\phi}\sin\frac{\theta}{2}\vec{1}_v \end{aligned} \tag{1}$$

The following table lists a number of easily recognized polarizations, their spherical coordinates on the Poincare sphere and the components of the polarization vectors, p_h and p_v.

Polarization	θ	ϕ	p_h	p_v
Horizontal	0	ϕ	1	0
Vertical	π	ϕ	0	$-e^{j\phi}$
In phase, 45°-linear	$\frac{\pi}{2}$	π	$\frac{1}{\sqrt{2}}$	$\frac{1}{\sqrt{2}}$
Out of phase, 45°-linear	$\frac{\pi}{2}$	0	$\frac{1}{\sqrt{2}}$	$\frac{-1}{\sqrt{2}}$
First Circular Polarization	$\frac{\pi}{2}$	$\frac{\pi}{2}$	$\frac{1}{\sqrt{2}}$	$-j\frac{1}{\sqrt{2}}$
Second Circular Polarization	$\frac{\pi}{2}$	$3\frac{\pi}{2}$	$\frac{1}{\sqrt{2}}$	$j\frac{1}{\sqrt{2}}$

2 Cross-Polarization Vector

Let $\vec{X}(\theta, \phi)$ be the polarization unit vector which is cross-polarized to $\vec{P}(\theta, \phi)$. The mapping of $\vec{X}$ onto the Poincare sphere is directly opposite to the map-

ping of $\vec{P}$ onto the sphere. Thus $\vec{X}$ is given by:

$$\vec{X}(\theta,\phi) = \vec{P}(\pi-\theta,\pi+\phi) \quad (2)$$

$$= \sin\frac{\theta}{2}\vec{1}_h + e^{j\phi}\cos\frac{\theta}{2}\vec{1}_v \quad (3)$$

3 Special Case

The special case of interest is the orthogonal set formed by the vertical and horizontal polarizations. Let $(\theta,\phi) = (0,0)$, then

$$\vec{P}(0,0) = \vec{1}_h \quad (4)$$

$$\vec{X}(0,0) = \vec{1}_v \quad (5)$$

Similarly, let $(\theta,\phi) = (\pi,\pi)$, then

$$\vec{P}(\pi,\pi) = \vec{1}_v \quad (6)$$

$$\vec{X}(\pi,\pi) = \vec{1}_h \quad (7)$$

4 Decomposition of a Vector

Let $\vec{B} = b_h\vec{1}_h + b_v\vec{1}_v$ be an arbitrary vector. It can be decomposed into a component with $\vec{P}(\theta,\phi)$ polarization and a component with $\vec{X}(\theta,\phi)$ polarization. Let these components be c_p and c_x, respectively. Thus:

$$\vec{B} = c_p\vec{P}(\theta,\phi) + c_x\vec{X}(\theta,\phi) \quad (8)$$

The components are obtained by the following dot products:

$$c_p = \vec{B}\bullet\vec{P}^*(\theta,\phi) \quad (9)$$

$$= \left[b_h\vec{1}_h + b_v\vec{1}_v\right]\bullet\left[\cos\frac{\theta}{2}\vec{1}_h - e^{-j\phi}\sin\frac{\theta}{2}\vec{1}_v\right]$$

$$= b_h\cos\frac{\theta}{2} - b_v e^{-j\phi}\sin\frac{\theta}{2} \quad (10)$$

$$c_x = \vec{B}\bullet\vec{X}^*(\theta,\phi) \quad (11)$$

$$= \left[b_h\vec{1}_h + b_v\vec{1}_v\right]\bullet\left[\sin\frac{\theta}{2}\vec{1}_h + e^{-j\phi}\cos\frac{\theta}{2}\vec{1}_v\right]$$

$$= b_h\sin\frac{\theta}{2} + b_v e^{-j\phi}\cos\frac{\theta}{2} \quad (12)$$

5 Change in Coordinate System Used in the Poincare Unit Sphere

As mentioned in Section 1, the mapping for two polarizations which are not cross-polarized must be specified in order for the mapping to be unique. The choice of which polarizations to use is arbitrary. In Section 1 the horizontal and in-phase, 45°-linear polarizations were used. It will become convenient in later sections to use $\vec{P}(\theta_0, \phi_0)$ and $\left(\frac{\vec{P}(\theta_0,\phi_0)+\vec{X}(\theta_0,\phi_0)}{\sqrt{2}}\right)$ for some θ_0 and ϕ_0, instead of the previously used polarizations.

Let (x', y', z') and $(1, \theta', \phi')$ be the cartesian and spherical coordinates of a point on the sphere in the new coordinate system. Let the new cartesian unit vectors be $\vec{1}_{x'}$, $\vec{1}_{y'}$ and $\vec{1}_{z'}$.

Let $\vec{P}(\theta_0, \phi_0)$ map to $(x', y', z') = (0, 0, 1)$ and let $\left(\frac{\vec{P}(\theta_0,\phi_0)+\vec{X}(\theta_0,\phi_0)}{\sqrt{2}}\right)$ map to $(x', y', z') = (1, 0, 0)$.

Note that

$$\begin{aligned}
\left(\frac{\vec{P}(\theta_0,\phi_0)+\vec{X}(\theta_0,\phi_0)}{\sqrt{2}}\right) &= \left[\frac{\cos\frac{\theta_0}{2}+\sin\frac{\theta_0}{2}}{\sqrt{2}}\right]\vec{1}_h - e^{j\phi}\left[\frac{\sin\frac{\theta_0}{2}-\cos\frac{\theta_0}{2}}{\sqrt{2}}\right]\vec{1}_v \\
&= \cos\left(\frac{\theta_0}{2}-\frac{\pi}{4}\right)\vec{1}_h - e^{j\phi_0}\sin\left(\frac{\theta_0}{2}-\frac{\pi}{4}\right)\vec{1}_v \\
&= \vec{P}(\theta_0 - \pi/2, \phi_0) \qquad \text{if } \theta_0 \geq \pi/2 \qquad (13) \\
&= \vec{P}(\pi/2 - \theta_0, \pi + \phi_0) \qquad \text{if } \theta_0 \leq \pi/2 \qquad (14)
\end{aligned}$$

The following relationships exist between the old and new unit cartesian vectors.

$$\begin{aligned}
\vec{1}_{x'} &= -\cos\theta_0\cos\phi_0\vec{1}_x - \cos\theta_0\sin\phi_0\vec{1}_y + \sin\theta_0\vec{1}_z \qquad (15) \\
\vec{1}_{y'} &= \sin\phi_0\vec{1}_x - \cos\phi_0\vec{1}_y \qquad (16) \\
\vec{1}_{z'} &= \sin\theta_0\cos\phi_0\vec{1}_x + \sin\theta_0\sin\phi_0\vec{1}_y + \cos\theta_0\vec{1}_z \qquad (17)
\end{aligned}$$

The following relationships exist between the old and new spherical coordinates.

$$\begin{aligned}
\sin\theta'\cos\phi' &= \cos\theta\sin\theta_0 - \sin\theta\cos\theta_0\cos(\phi - \phi_0) \qquad (18) \\
\sin\theta'\sin\phi' &= -\sin\theta\sin(\phi - \phi_0) \qquad (19) \\
\cos\theta' &= \cos\theta\cos\theta_0 + \sin\theta\sin\theta_0\cos(\phi - \phi_0) \qquad (20)
\end{aligned}$$

6 Nulling Algorithm

Consider a measured signal $\vec{T}$ which contains a user signal, $\vec{U}$, of known polarization $\vec{P}(\theta_0, \phi_0)$ but unknown amplitude, a and phase, γ, and a jammer signal, $\vec{J}$, of known amplitude n but unknown phase ψ and unknown polarization. Let the measured horizontal and vertical components of the total signal be t_h and t_v, respectively. The vector representation of the measured signal is given below:

$$\vec{T} = t_h \vec{1}_h + t_v \vec{1}_v \quad (21)$$

$$= \vec{U} + \vec{J} \quad (22)$$

6.1 1st Step: Decomposition into Co- and Cross-polarizations

The first step in the algorithm is to decompose the measured signal into components co-polarized with the known user polarization and cross-polarized to it.

Let the amplitude and phase of the component of the jammer signal co-polarized with the user signal be n_c and ψ_c, respectively. Let the amplitude and phase of the component of the jammer signal cross-polarized with the user signal be n_x and ψ_x, respectively. The vector representation of the jammer, user and total signals is given below.

$$\vec{J} = n_c e^{j\psi_c} \vec{P}(\theta_0, \phi_0) + n_x e^{j\psi_x} \vec{X}(\theta_0, \phi_0) \quad (23)$$

$$\vec{U} = a e^{j\gamma} \vec{P}(\theta_0, \phi_0) \quad (24)$$

$$\vec{T} = \left(a e^{j\gamma} + n_c e^{j\psi_c}\right) \vec{P}(\theta_0, \phi_0) + n_x e^{j\psi_x} \vec{X}(\theta_0, \phi_0) \quad (25)$$

$$= t_c \vec{P}(\theta_0, \phi_0) + t_x \vec{X}(\theta_0, \phi_0) \quad (26)$$

where

$$n^2 = n_c^2 + n_x^2 \quad (27)$$

$$t_c = a e^{j\gamma} + n_c e^{j\psi_c} \quad (28)$$

After the decomposition, the values of n_x, ψ_x and n_c are known. The total co-polarized signal, t_c, is also known. However, there are three unknowns, i.e., ψ_c, a and γ. There is not enough information in the value for t_c to identify the unknowns.

6.2 2nd Step: Isolation of the Jammer's Polarization

In this section, the mapping to the Poincare sphere and the primed coordinate systems outlined in Section 5 are used for convenience.

Since n_c and n_x are known, the polarization of the jammer will map onto a circle on the Poincare sphere. This circle is defined by

$$\theta' = \theta'_j = 2\cos^{-1}\left(\frac{n_c}{n}\right) = 2\sin^{-1}\left(\frac{n_x}{n}\right) = 2\tan^{-1}\left(\frac{n_x}{n_c}\right) \quad (29)$$

Consider the signals that are found by decomposing the total signal into components co- and cross-polarized to a polarization with this θ' coordinate but arbitrary ϕ' coordinate. This is shown below:

$$\vec{T} = \left[\vec{T} \bullet \vec{P}^*(\theta'_j, \phi')\right] \vec{P}(\theta'_j, \phi') + \left[\vec{T} \bullet \vec{X}^*(\theta'_j, \phi')\right] \vec{X}(\theta'_j, \phi') \quad (30)$$

In particular, consider the cross-polarized component

$$\begin{aligned}
\vec{T} \bullet \vec{X}^*(\theta'_j, \phi') &= (\vec{U} + \vec{J}) \bullet \vec{X}^*(\theta'_j, \phi') \\
&= \left[\left(ae^{j\gamma} + n_c e^{j\psi_c}\right) \vec{P}(\theta_0, \phi_0) + n_x e^{j\psi_x} \vec{X}(\theta_0, \phi_0)\right] \\
&\quad \bullet \left[\sin\frac{\theta'_j}{2} \vec{P}^*(\theta_0, \phi_0) - e^{-j\phi'} \cos\frac{\theta'_j}{2} \vec{X}^*(\theta_0, \phi_0)\right] \\
&= \left(ae^{j\gamma} + n_c e^{j\psi_c}\right) \sin\frac{\theta'_j}{2} - n_x e^{j\psi_x} e^{-j\phi'} \cos\frac{\theta'_j}{2} \\
&= \left(ae^{j\gamma} + n_c e^{j\psi_c}\right) \frac{n_x}{n} - \frac{n_c n_x}{n} e^{j\psi_x} e^{-j\phi'} \quad (31) \\
&= t_c \frac{n_x}{n} - t_x \frac{n_c}{n} e^{j\phi'} \quad (32)
\end{aligned}$$

The resultant phasor is comprised of two parts. The first part is independent of the variable ϕ' while the second has a $e^{-j\phi'}$ dependence. Note that there seems to be no new information here since t_c, t_x, n_c, n_x and n are already known.

An alternate calculation is given below.

Let the unknown, ϕ' spherical coordinate of the jammer's polarization be ϕ'_j. The jammer's polarization is given by $\vec{P}(\theta'_j, \phi'_j)$.

$$\begin{aligned}
\vec{T} \bullet \vec{X}^*(\theta'_j, \phi') &= (\vec{U} + \vec{J}) \bullet \vec{X}^*(\theta'_j, \phi') \\
&= ae^{j\gamma} \vec{P}(\theta_0, \phi_0) \bullet \vec{X}^*(\theta'_j, \phi')
\end{aligned}$$

$$+ne^{j\psi}\vec{P}(\theta'_j,\phi'_j)\bullet\vec{X}^*(\theta'_j,\phi') \tag{33}$$

$$\begin{aligned}
\vec{T}\bullet\vec{X}^*(\theta'_j,\phi') &= ae^{j\gamma}\sin\frac{\theta'_j}{2} \\
&\quad +ne^{j\psi}\left[\cos\frac{\theta'_j}{2}\vec{P}(\theta_0,\phi_0)+e^{j\phi'_j}\sin\frac{\theta'_j}{2}\vec{X}(\theta_0,\phi_0)\right] \\
&\quad \bullet\left[\sin\frac{\theta'_j}{2}\vec{P}^*(\theta_0,\phi_0)-e^{-j\phi'}\cos\frac{\theta'_j}{2}\vec{X}^*(\theta_0,\phi_0)\right] \\
&= ae^{j\gamma}\sin\frac{\theta'_j}{2}+ne^{j\psi}\cos\frac{\theta'_j}{2}\sin\frac{\theta'_j}{2}\left[1-e^{j(\phi'_j-\phi')}\right] \\
&= \frac{n_x}{n}\left\{ae^{j\gamma}+n_ce^{j\psi}\left[1-e^{j(\phi'_j-\phi')}\right]\right\} \qquad (34)
\end{aligned}$$

6.3 If user amplitude, a, is known

In this section it will be shown that if the user amplitude is also known, it is possible to further identify the user's phase, γ. Two possible solutions for this phase can be found.

From Equation 28 we will define the phase α_c.

$$\begin{aligned}
t_c &= ae^{j\gamma}+n_ce^{j\psi_c} &(35)\\
&= |t_c|e^{j\alpha_c} &(36)\\
& &(37)
\end{aligned}$$

All the variables in the above equation except γ are known. Thus,

$$\begin{aligned}
\gamma &= \alpha_c \pm \cos^{-1}\left[\frac{a^2+|t_c|^2-n_c^2}{2a|t_c|}\right] &(38)\\
\psi_c &= \alpha_c \mp \cos^{-1}\left[\frac{n_c^2+|t_c|^2-a^2}{2n_c|t_c|}\right] &(39)\\
\phi'_j &= \psi_x-\psi_c \\
&= \psi_x-\alpha_c\pm\cos^{-1}\left[\frac{n_c^2+|t_c|^2-a^2}{2n_c|t_c|}\right] &(40)
\end{aligned}$$

The uncertainty in the selection of γ comes from the selection of the correct sign of the arccos function.

Rome Laboratory

Customer Satisfaction Survey

RL-TR-_____

Please complete this survey, and mail to RL/IMPS, 26 Electronic Pky, Griffiss AFB NY 13441-4514. Your assessment and feedback regarding this technical report will allow Rome Laboratory to have a vehicle to continuously improve our methods of research, publication, and customer satisfaction. Your assistance is greatly appreciated.
Thank You

_____

_____

Organization Name:_____(Optional)

Organization POC: _____(Optional)

Address:_____

1. On a scale of 1 to 5 how would you rate the technology developed under this research?

5-Extremely Useful 1-Not Useful/Wasteful

Rating_____

Please use the space below to comment on your rating. Please suggest improvements. Use the back of this sheet if necessary.

2. Do any specific areas of the report stand out as exceptional?

Yes___ No_____

If yes, please identify the area(s), and comment on what aspects make them "stand out."

3. Do any specific areas of the report stand out as inferior?

Yes___ No___

If yes, please identify the area(s), and comment on what aspects make them "stand out."

4. Please utilize the space below to comment on any other aspects of the report. Comments on both technical content and reporting format are desired.

*U.S. GOVERNMENT PRINTING OFFICE: 1995-610-126-20034